Development of a Hygroscopicity Tandem Differential Mobility Analyzer and Use
for Laboratory and Field Measurements

University of Aegean

Department of Environment

Giamarelou Maria

May 2011

Development of a Hygroscopicity Tandem Differential Mobility Analyzer and Use
for Laboratory and Field Measurements

University of Aegean

Department of Environment

Giamarelou Maria

May 2011

Far better an approximate answer to the right question,

which is often vague,

than an exact answer to the wrong question,

which can always be made precise.

John W. Tukey, 1962

Abstract

Fine and ultrafine particles in the atmosphere are of interest because of their effects on the earth's radiation budget, visibility impairment, and human health. These effects depend on particle size, morphology, and composition. Various instruments and techniques have been developed for size distribution measurements. The most efficient way of measuring the size distribution of ultrafine particles is by determing their electrical mobility. The most widely used arrangement of doing that is a Differential Mobility Analyzer (DMA). Conventional DMAs for classification of aerosol particles have one polydisperse-particle inlet and one monodisperse-particle outlet. As a result, when they are used as particle classifiers in aerosol-mobility spectrometers it is required to scan through different operating conditions, thereby requiring a significant amount of time (i.e., of the order of a minute) for a single mobility distribution measurement. DMAs with multiple outlets can significantly reduce this scanning time since particles of different mobility can be classified and detected simultaneously. In addition, depending on the relative location of the first and the last outlet from the inlet, one can increase the dynamic mobility range of the selected particles in a single particle mobility distribution measurement. Overlap of particle mobilities selected by the different exits can also provide valuable information for improving the inversion of the measured signal to particle size distributions. Tandem DMA systems are also used for probing size-changing properties of aerosol particles that can define their effects on climate and human health (e.g., water adsorption and condensation on the particles). Inversion techniques are needed for retrieving the both size distribution (using a single DMA in mobility spectrometers) and the size-changing properties (using Tandem DMA systems, TDMA) of the sampled aerosol. The proposed project will yield a novel DMA system, which will be used as classifier in mobility spectrometers and TDMA systems.

Contents

List of Tables

List of Figures

CHAPTER 1.   INTRODUCTION

CHAPTER 1. INTRODUCTION

Fine and ultrafine particles in the atmosphere are of interest because of their effects on the earth's radiation budget (IPCC, 2007), visibility impairment (NRC, 1993), and human health (e.g. Oberdörster, 2000; Peters et al., 1997). These effects depend on particle size, morphology, and chemical composition. Depending on the size range of the sample particles, a range of methods can be employed to measure the size distribution of the particles. Different measurement methods provide different measures of particle size. Thus, for example, typical atmospheric particles of the equivalent size (e.g., equivalent volume diameter) can have different optical diameter (Covert *et al*. 1990; Dick and McMurry 2007; Dockery and Pope 1994; Heintzenberg et al. 2002; Heintzenberg et al. 2004; Hering and McMurry 1991; Naoe and Okada 2001; Okada and Heintzenberg 2003), masses (Geller et al. 2006; McMurry et al. 2002), and aerodynamic diameter (DeCarlo et al. 2005; McMurry et al. 2002), indicating that they are chemically and/or morphologically different. Recent studies on tandem measurements of multiple particle properties have begun to provide information for the relationships between the particle chemical and physical properties. This research focuses on tandem measurements for which particles are first classified based on their electrical mobility with Differential Mobility Analyzers (DMAs) (Hewitt, 1957; Liu and Pui, 1974; Knutson and Whitby, 1975; Chen et al., 1998)

The DMA (Hewitt, 1957) has been widely applied in a variety of aerosol measurement applications including the generation of monodisperse aerosol standards for instrument calibration (Liu and Pui, 1974) and the measurement of submicron aerosol size distributions (Knutson, 1976; Hoppel, 1978; Fissan *et al*., 1982; Plomp *et al*., 1982; Scheibel *et al*., 1983; Kousaka *et al*., 1985). The use of two DMAs in series, referred to as a tandem differential mobility analyzer (TDMA) system, has, also, been reported. Liu *et al*. (1978) used the TDMA to examine the deliquescent and hygroscopic properties of monodisperse aerosols, and McMurry et al. (1983) measure the reaction rate between ammonia gas and sulfuric acid aerosol droplets using a TDMA. The most widespread application is TDMA is that of the hygroscopicity (H-TDMA), where the dry selected particles are exposed to a well-defined relative humidity (RH) conditions, in order to measure hygroscopic growth of the particles (e.g. Gysel *et al*., 2002; Rader and McMurry, 1986; Swietlicki *et al*., 2008). Rader *et al*. (1986b) also used the TDMA to measure evaporation rates of several organic aerosol materials. Joutsensaari *et al*. (2001) have developed an organic O-TDMA in order to determine the affinity of particles to different

organic species by exposing them to, e.g., subsaturated ethanol vapours. Moreover, evaporation rates of volatile particles at ambient temperature have been determined by employing laminar flow cells between the two DMAs (e.g., Bilde & Pandis, 2001; Dassios & Pandis, 1999). The volatility V-TDMA technique is used to measure the amount of refractory material in aerosol particles (e.g. Paulsenet *et al*., 2006; Philippin *et al*., 2004), while a combined volatilization humidification, VH-TDMA, system has been used to investigate the contributions of different constituents in mixed particles to the hygroscopic water uptake (e.g., Johnson *et al*., 2004). Figure 1.1 illustrates an overview of the concept behind the tandem measurements.

Particles separated based on their electrical mobility in mobility spectrometers have to be further analyzed to obtain the size distribution of the particles. In an ideal situation, one-to-one correspondence between the channels and size classes, i.e. particles in a certain size range would be collected entirely in a particular channel, with particles in a neighboring size range being collected in a neighboring channel, with no overlap whatsoever, is the desired outcome. However, no aerosol spectrometer behaves in this idealized manner. Typically, a particular channel will collect particles from multiple size ranges due to particle diffusivity within the DMA and the number of charges they carry. Thus, a degree of indeterminacy is introduced into the interpretation of the measurements, so that a continuous size distribution now has to be estimated from a set of discrete measurements, each of which is influenced by all values of the unknown distribution, i.e. "the set of numbers which comprises the answer must be 'unraveled', as it were, from a tangled set of combinations of these numbers", (Twomey, 1977).

The main goal of this study is to provide the necessary tools for interpreting size distribution measurements from electrical mobility spectrometers and TDMA systems. To achieve that I will develop the mathematical framework for describing the performance of the DMA and extend it for a novel design. More specifically I will design and model the performance of a Multiple Monodisperse Outlet DMA (MMO-DMA), and design a DMA with two monodisperse outlets (i.e., the Dual-MO-DMA). After that I will develop the necessary data inversion algorithms for both the Scanning Mobility Particle Spectrometer (SMPS) and the TDMA that will include a Dual-MO-DMA and use it for field and laboratory measurements.

The following sections provide a brief review of the phenomena and processes involved in differential mobility analysis, the state of art in DMA instrumentation and describe a

number of inversion techniques that grapple with this problem in different ways and with differing levels of success.

```
┌─────────────────────────────────────────────────────────────────────┐
│ ┌─────────────────────────────┐                                       │
│ │ Particle Classiffication    │                                       │
│ └─────────────────────────────┘                                       │
│     • DMA                                                             │
│     • TDMA                                                            │
└─────────────────────────────────────────────────────────────────────┘
┌─────────────────────────────────────────────────────────────────────┐
│ ┌─────────────────────────────┐                                       │
│ │ Physicochemical properties  │                                       │
│ └─────────────────────────────┘                                       │
│     • APM (mass, e.g. Ehara et al., 1996)                             │
│     • ATOFMS, AMS (Composition, vacuum aerodynamic diameter, e.g. Gard│
│       et al., 1997)                                                   │
│     • CCN (Cloud activation, e.g. Delene & Deshler,2000; Hudson, 1989;│
│       Roberts & Nenes, 2005)                                          │
│     • MALS (Angular light scattering, e.g. Dick & McMurry,2007; Dick  │
│       et al., 1998; Wyatt et al., 1988)                               │
│     • Impactor (Aerodynamic Size, composition, e.g. Hering et al., 1977;│
│       Hering & Friedlander, 1979; Marple et al., 1991)                │
│     • OPC (Light scattering, e.g. Cooke & Kerker, 1975; Heyder & Gedhart,│
│       1979; Liu & Daum, 2000; Szymanski & Liu,1986)                   │
│     • TEM (Morphology, e.g. Park et al., 2004a, 2004b)                │
└─────────────────────────────────────────────────────────────────────┘
```
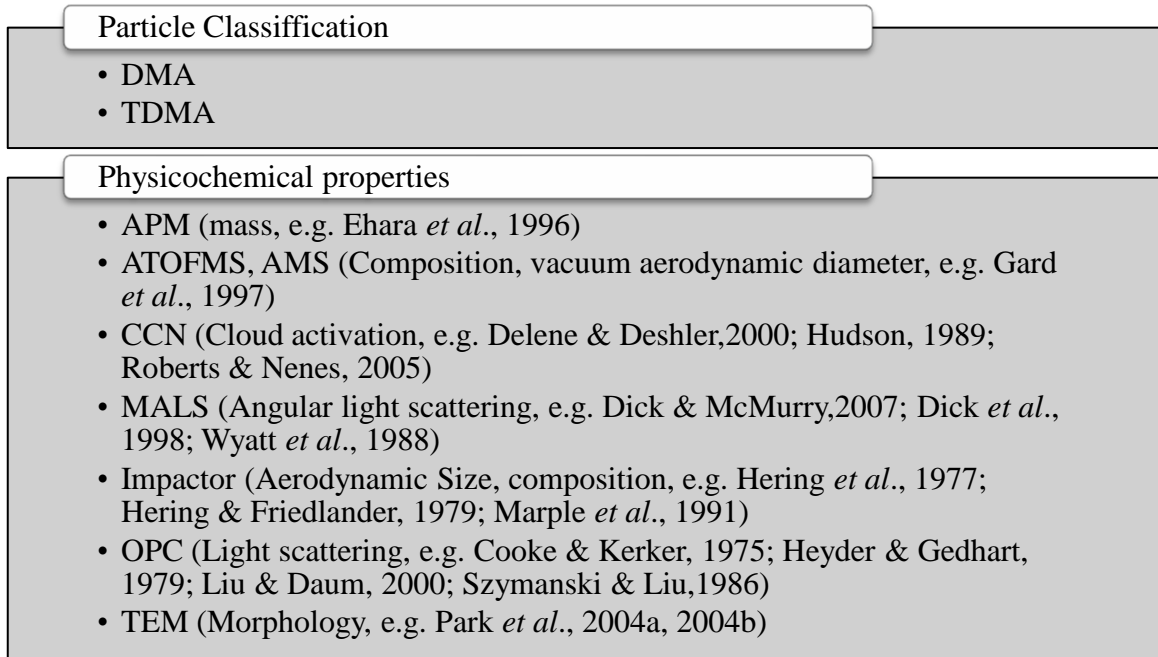
Figure 1. 1 Schematic of aerosol tandem measurements. Particles of a given mobility diameter are selected by a DMA (or TDMA so as to process the aerosol prior the additional measurements) from the sampled aerosol. Additional information about the physicochemical properties is obtained from one or more additional measurement methods in series.

CHAPTER 2. LITERATURE REVIEW

CHAPTER 2. LITERATURE REVIEW

This Chapter describes the fundamental concepts and theories needed to understand the operation of the electrical mobility spectrometers and Tandem Differential Mobility Analyzer (TDMA) systems.

The first Section of the Chapter covers some fundamental properties of particles and aerosols. The second Section presents a brief review of the most widely accepted theories that describe diffusion charging of aerosol particles. In the third Section Fundamental concepts of aerosol classifiers such as their transfer function and resolution are presented, while the fourth Section describes briefly the electrical mobility measurement method used to detect particles in such instruments. The last Section gives a definition of the instrument's kernel and introduces the problem of data inversion for aerosol analyzers, viz., the techniques used to translate the electrical mobility measurements to aerosol size distributions.

2.1 Aerosol Particle Properties – Size and Size Depended Properties

The term aerosol is used by definition to refer to an assembly of liquid or solid particles suspended in a gaseous medium in the size range of 1 nm to 100 μm (Baron and Willeke, 2001). Particles either manufactured or naturally produced have a great diversity in size, morphology, chemical composition. Even if the particles under examination have the same microscopically observed diameter, the mass, the surface, the chemical composition and other properties may differ markedly. A variety of techniques is available for obtaining useful information about particles, such as their size which is the most important parameter describing aerosol behavior.

A commonly used term is that of the *equivalent diameter*, i.e. the diameter of a sphere having the same value of a specific physical property as the irregularly shaped particle being measured (Fig. 2.1). Thus, the *mobility equivalent diameter*, d_B, is defined as the diameter of a sphere with the same mobility as the particle in question, while the *aerodynamic equivalent diameter*, d_a, is the diameter of a standard-density sphere having the same gravitational settling velocity as the particle being measured (Baron and Willeke, 2001). For particles with complex shape such as an agglomerate, a significant part of the internal volume is made of voids, in such particles are defined the *mass equivalent diameter*, for which the particle is compressed into a spherical particle without voids and the *envelope equivalent diameter*, for which the particle voids are included in the sphere.

5

When observing a particle's shape with a microscope and calculating the diameter of a circle that has the same area we can derive the *projected area equivalent diameter* is. For particles of submicrometer size we can also define a *diffusion equivalent diameter*, i.e. the diameter of a standard-density spherical particle with the same rate of diffusion as the particle measured. In a similar manner, one can define the *electrical mobility equivalent diameter* of a charged particle moving in an electric field (Baron and Willeke, 2001). The aerodynamic diameter is used for particles in the inertial size range, i.e. larger than 0.5 μm, while for particles smaller than 0.5 μm undergoing diffusion, the diffusion diameter is used (Walter, 2001).
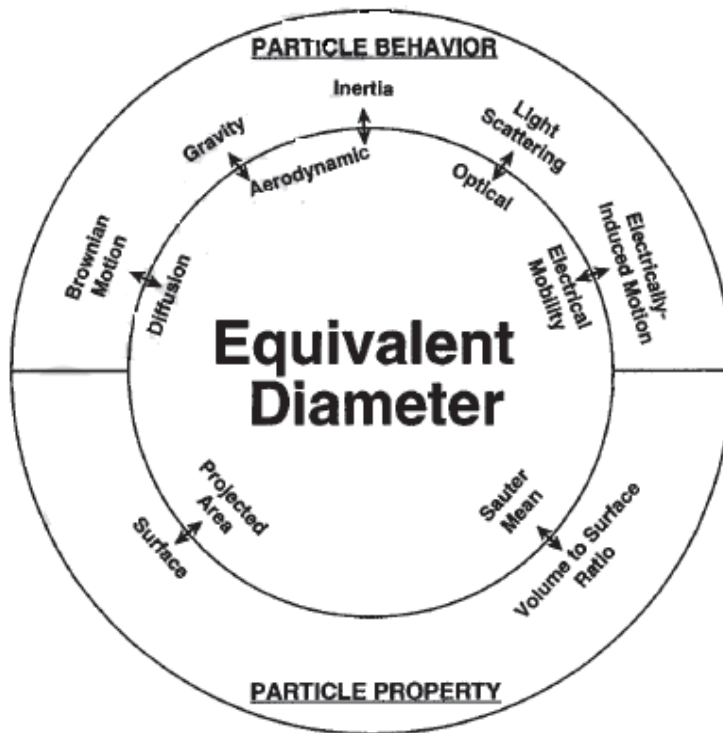
Figure 2. 1 Particle size definitions that depend on observations of particles or behavior

Aerosols almost never consists of particles having the same size. Such an aerosol would be said to be monodisperse. The most highly monodisperse aerosols are those generated in a laboratory, with a spread in particle diameter of a few percent. Conventionally, a distribution with a spread of less than about 10% to 20% is considered monodisperse. Thus, aerosols with a large range in size are defined as polydisperse.

Both monodisperse and polydisperse aerosols consist of particles with sizes distributed over a certain range. A histogram would be the simplest size distribution of the number of

particles in successive size intervals. If the intervals become sufficiently fine, the distribution would become a differential size distribution. The dependent variant is the number of particles, $N(d_p)$, in the size interval from d_p to dd_p, thus, is called a number distribution defined as $dN = N(d_p)dd_p$, where d_p is the particle diameter. As the particle diameter typically ranges over several orders of magnitude, is useful to use $dlnd_p$ for the size interval, thus the size distribution becomes $dN = N(d_p)dlnd_p$. It has been found that aerosol size distributions from many different sources follow the lognormal distribution given by: $dN = \frac{N}{\sqrt{2\pi}\ln\sigma_g}exp\left(\frac{-(\ln d_p - \ln CMD)^2}{2(\ln\sigma_g)^2}\right)dlnd_p$, where N is the total number of particles, is the count median diameter (CMD) by number – which is equal to the geometric mean diameter, d_g, for a lognormal distribution – and σ_g is the geometric standard deviation, given by: $\ln\sigma_g = \left[\frac{\int_0^\infty (\ln d_p - \ln d_g)^2 dn}{N-1}\right]^{1/2}$.

Apart from the widely used lognormal function for particle size distributions, the modified gamma distribution has been also used for atmospheric aerosols (Pruppacher and Klett, 1980). According to Brown and Wohletz (1995) the Weibull distribution fits fragmentation aerosols somewhat better than the lognormal distribution. Similar to the Weibull distribution is the Rosin-Rammler (1933) distribution.

Size range of the aerosol is one of the factors to consider in the selection of instrumentation for aerosol measurements. There is a continual effort from aerosol measurement researchers to build aerosol instruments that measure one or more aerosol properties over a wider size range. Another factor to take in consideration is the in-situ or ex-situ measurement. There are two approaches, namely the collection and analysis approach or direct-reading sensors. Figure 2.2 shows an overview of the size range of several types of commonly used classes of instruments.

Other important properties of aerosol particles that are of high relevance to atmospheric aerosols, are the hygroscopicity (i.e., the ability of the particles to adsorb and condense water vapor), and the volatility of aerosol particles. These properties can give an indirect indication of the composition of the particles. Atmospheric aerosols are typically hygroscopic and can condense water at subsaturated conditions. Hygroscopic growth of the particles at intermediate relative humidity (RH) conditions can influence the light scattering by the particles, their potential to act as cloud condensation nuclei, and their

chemical reactivity. The RH dependence of light scattering is one of the parameters needed to estimate the direct climate forcing by aerosol particles. Because of that the dry aerosol particle size distribution and the size-dependent water uptake at different RH conditions must be known to model the humidity dependence of the light scattering of an aerosol. Efforts are currently undertaken to include the effects of hygroscopic growth of aerosol particles in global climate models in order to better predict their scattering properties and size under varying humidity conditions (Randall *et al*., 2007). The two most widely used techniques enabling measurement of the change in the amount of water absorbed to an aerosols particle with varying RH are the single aerosol particle levitation technique using an electrodynamic balance (EDB; Tang and Munkelwitz, 1993) and the hygroscopicity tandem differential mobility analyser technique (HTDMA; Liu *et al*., 1978; Rader and McMurry, 1986; Swietlicki *et al*., 2008). The EDB technique, which measures the properties of individual super-micrometer aerosol particles, is suitable for laboratory measurements. The HTDMA technique, which probes the hygroscopicity of all aerosol particles of a well-defined dry diameter at once, is suitable for field and laboratory measurements. HTDMA instruments cover the sub-micrometer diameter range, which includes the majority of the atmospheric aerosol particles.
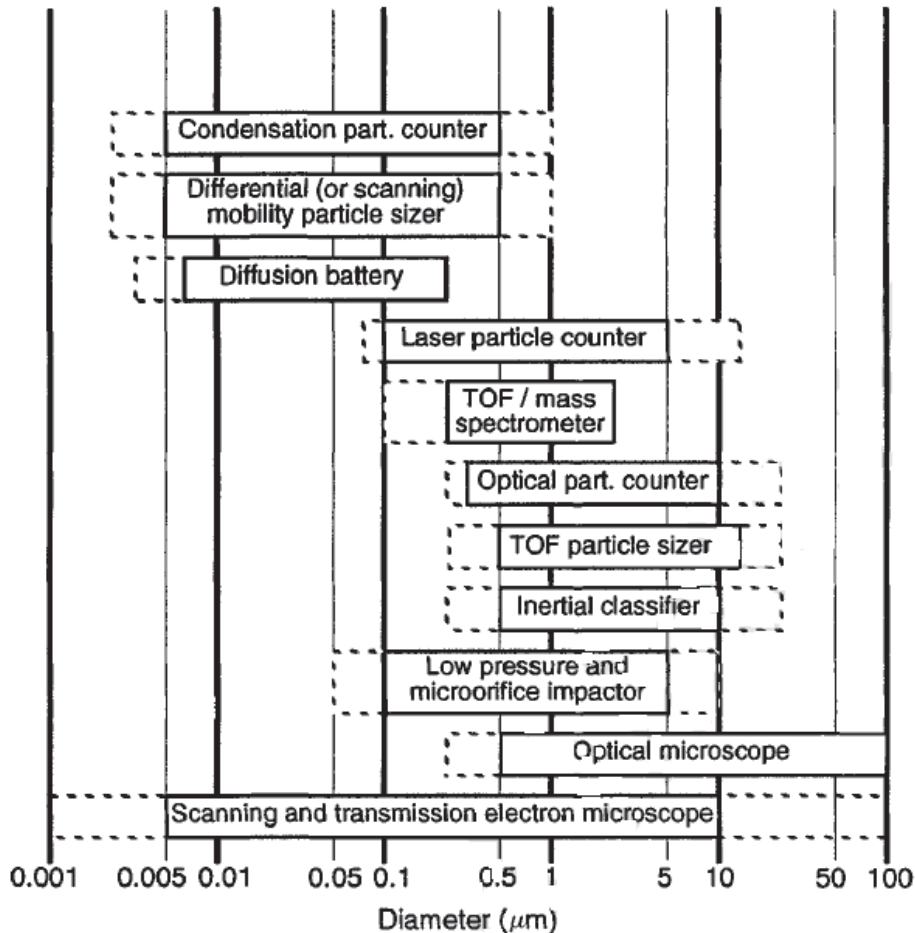
Figure 2. 2 Measurement size range of some principal aerosol sizing and analytical instruments. (Adapted from Pui, 1996.)

2.2 Electrical Mobility Measurements

2.2.1 Diffusion Charging of Particles

Aerosol particles are readily charged during generation by a variety of charge emission mechanisms or by the attachment of gas ions. The principal method for sizing ultrafine particles is based on knowing the charge distribution of the charged particles and determining the electrostatic force that can be applied to such particles in electrical mobility analyzers.

Large particles frequently acquire multiple charges, but as the probability of charging decreases with decreasing particle size, sufficiently small particles will carry only one elementary unit of charge so that the charge on that particle is $q = \pm e$. If a charged particle is placed in an electric field of known strength, it will migrate with a velocity that depends only on the particle size and structure, allowing the determination of the particle size. Besides the fact that such particles have relatively high diffusivities, measuring their size

9

with high resolution is possible as the forces imparted on them can be sufficiently large to overwhelm diffusional effects.

The distribution of charges on particles with respect to size and among particles of a given size must be known to accurately determine the particle size distribution by measuring their electrical mobility. Typically, few ultrafine particles acquire a charge, so the particles with a given velocity will account for only a small fraction of the total particles of a given size. Because of the increasing probability of a particle acquiring multiple charges with increasing size, the migration velocities of large particles can vary from particle to particle, so migration-based particle size analysis is generally limited to particles smaller than about 1 μm in diameter. Even at that size, the finite probability of multiple charging complicates data analysis.

2.2.1.1 Behavior of Charged Particles

When a particle with charge q moves in an electric field of strength E, it experiences a force $F = qE$. Because of the low ion densities and slow charge transfer kinetics in ambient temperature gases, aerosol particles usually carry only a small number of elementary charges. Thus, the charge is represented as $q = ne$, where $e = 1.609 \; x \; 10^{-19}$ Coulomb is the elementary unit of charge and n is the number of charges that a particle carries. For migration times that are long compared to the aerodynamic relaxation time, $\tau_a = m_p B$ a charged particle will migrate at a steady-state migration velocity relative to the gas motion of $v_e = Z_p E$, where B and Z_p are the mechanical and electrical mobilities of the particle, respectively. The electrical mobility of spherical particles with diameter d_p in the Stokes regime, is given by the equation $Z_p = \frac{neC_c(K_n)}{3\pi\eta d_p}$, where η is the gas viscosity, C_c is the Cunningham slip correction factor that accounts for noncontinuum effects when the particle size becomes comparable with or smaller than the mean free path of the gas molecules, λ, or in dimensionless terms, when the Knudsen number, i.e. $K_n = \frac{2\lambda}{d_p}$, becomes large. The slip correction factor is given by $C_c = 1 + K_n \left(\alpha + \beta exp \left(-\frac{\gamma}{K_n} \right) \right)$, where the empirically determined coefficients are $\alpha = 1.142$, $\beta = 0.558$, $\gamma = 0.999$ (Allen and Raabe, 1985).

Figure 2.3 shows the variation of the electrical mobility with particle size under normal ambient atmospheric conditions for particles carrying different numbers of elementary

number of charge. Because of the dependence of the mobility on particle size, $Z_p \propto d_p^{-1}$, the range of electric field strengths required to classify particles throughout the submicron size range exceeds the capabilities of a single instrument operating at fixed flow rates (Flagan, 2001).

In general, mobility sizing techniques are applied to small particle migrating in an electric field. Consider particles (Fig 2.4) that migrate a distance b under the action of an applied electric field, E, produced by applying a voltage difference V over the distance b. The time required to migrate that distance is $\tau = \frac{b}{Z_p E}$. The particle diffusivity is related to the mobility by the Einstein relation $D = BkT$, where k is the Boltzmann constant and T is the temperature. The ratio of the migration distance to the root mean square displacement due to Brownian diffusion during particle migration, i.e. $\langle x^2 \rangle^{1/2} = \sqrt{2Dt}$, is given by the equation $\frac{b}{\langle x^2 \rangle^{1/2}} = \sqrt{\frac{neV}{2kT}}$. For large voltages, migration will dominate, while for small applied voltages diffusion will distort the response of any mobility-based particle measurement. The voltage that is required for a given measurement depends on the desired mobility or size resolution. Electrostatic breakdown within the apparatus limits the maximum operating voltage and, therefore, the highest attainable resolution (Flagan, 2001).
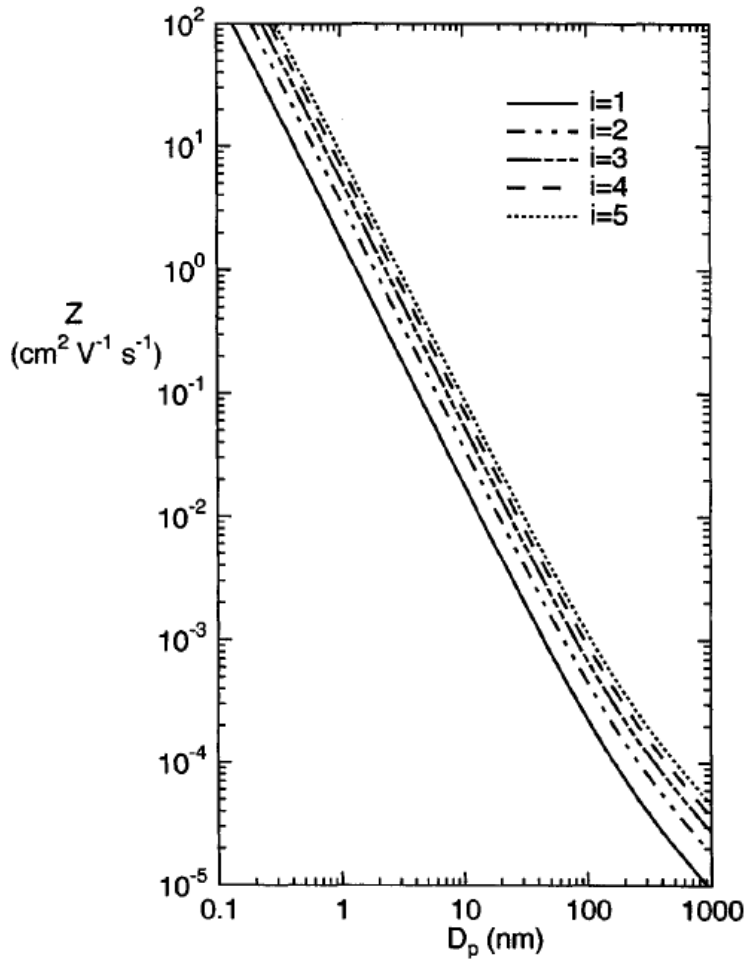
Figure 2. 3 Variation of mobility with size for particles with different charge.
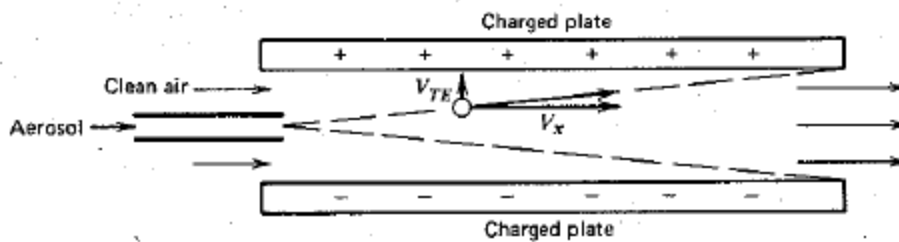
Figure 2. 4 Diagram of a simple electrical mobility analyzer (adopted from Hinds, 1999)

2.2.1.2 Unipolar and Bipolar Diffusion Charging

Accurate determination of the size of the particle from measurements of the electrical mobility presupposes knowledge of the number of charges on the classified particle, while measurement of the size distribution also requires that the fraction of particles of a given size that carry a given number of charges be accurately known. Hence, the production of aerosol particles with a known charge distribution is critical for electrical mobility measurements.

The charge distribution of sampled aerosol particles cannot be accurately known. For this reason the aerosol must be conditioned to a known charge state. The diffusion charge is unipolar or bipolar depending on the polarity of the ions in the gas, i.e. only positive or negative ion, or both kinds, respectively (Other mechanisms of charging aerosol particles are discussed in Hinds (1999) § 15.4 and Flagan (2001)). As the equilibrium charge distributions can be determined from well-established thermodynamic considerations, they are preferred. The process of charge transfer between the aerosol and an electrically neutral cloud of positive and negative ions is called bipolar diffusion charging. Aerosols that have undergone bipolar diffusion charging consist of positively and negatively charged particles. Even though, a well-characterized charge distribution is produced, at the small end of the electrical mobility sizing range only a tiny fraction of particles acquire any change.

After long exposure of the particles to bipolar ion mixtures, frequent ion-particle collisions will bring the particles to a state of charge equilibrium. Then the fraction of particles of diameter d_p that carry n charges is described by the Boltzmann charge distribution (Flagan, 2001), i.e., $f_n = \dfrac{exp\left(-\frac{n^2}{2\sigma^2}\right)}{\sum_{k=-\infty}^{\infty} exp\left(-\frac{k^2}{2\sigma^2}\right)}$. Boltzmann's law is commonly used to predict the charge distribution on the particles (Gunn (1955); Takahashi (1971); Liu & Pui (1974a;b). After exposure to a bipolar ion mixture, the aerosol charge distributions asymptotically approaches a steady state, which although similar to Boltzmann charge distribution, is generally asymmetrical due to differences in the properties of positive and negative ions. When the concentrations of positive and negative ions differ markedly, this asymmetry increases. The fact that in common bipolar gases mobility of negative ions is higher compared to that of positive ions (cf. Zeleny (1929); Mohnen (1977)) results in a slightly asymmetric particle charge distribution as indicated by many researchers (Fuchs & Lissowski (1956); Clement & Harrison (1991)). The extreme limit of unipolar charging occurs when the aerosol is exposed only to ions of one polarity. In unipolar diffusion charging the number of charges increases with time while the charging rate reduces since fewer ions have sufficient thermal energy to overcome the repulsive force and collide with the particle. The methods usually used to charge aerosol particles for mobility analysis corona discharge (White, 1951), radioactive decay (Liu and Pui, 1974b), photoelectron emission (Schmidt-Ott et al., 1980), and droplet formation in the presence of an electric field.

A gas usually contains a few free electrons and a comparable number of positive ions. At sufficiently high electric fields, the free electrons can be accelerated to sufficiently high velocities that their collisions with gas molecules lead to the ejection of additional electrons. A cascade of such events, called an *electron avalanche*, creates the corona and generates large numbers of positive ions and free electrons in the gas. The corona may be either positive or negative, which is generally more stable. The positive corona does not require an electron-absorbing gas and is frequently used to charge aerosol particles for measurement and has also been used in numerous electrostatic precipitators and the original electrical aerosol analyzer charger (Figure 2.5). In that charger, the corona is operated with a potential between a central wire and a coaxial screen. The aerosol passes between that screen, which is maintained at a small positive voltage and a coaxial electrode so that charging takes place in a region of weak electric field and charged particle losses due to migration to the wall are minimized. Hewitt (1957) introduced an alternating potential in the outer region to reverse the migration of charged particles and further reduce their deposition, an approach employed, again, recently, in efforts to improve the efficiency of unipolar charging of particles in the low nanometer size range (Buscher et al., 1994).

Commonly aerosol neutralizers employed in mobility spectrometers use radioactive bipolar diffusion chargers. In a typical aerosol device, the gas flows through a chamber that contains a small radioactive source, such as that shown in Figure 2.6, when the aerosol is passed near this source the air is ionized and the aerosol particles become charged. A number of different isotopes have been used in aerosol neutralizers and chargers.

The earliest theoretical description of this charging (Lissowski, 1940) indicated that the charge distribution would eventually equilibrate so as to obey Boltzmann's law given by:

$$\phi_v(d_p) = (2\pi\alpha)^{-1/2}exp(-v^2/2\alpha) \qquad\qquad (1)$$

where $\phi_v(d_p)$ is the fraction of particles with diameter d_p carrying v elementary charges, $\alpha = \frac{d_p kT}{2e^2}$, k is the Boltzmann's constant and T is the absolute temperature, e the charge of electron. Liu and Pui (1974c) and Kojima (1978) have experimentally verified Eq. 1 for particle sizes from 0.02 to 1.0 μm diameter for radioactive chargers of the same type and strength as in the TSI instrument. Experiments by Pollak and Metnieks (1962) and by Kojima (1978) for particles below 0.02 μm, indicate that Eq. 1 underestimates the number of charged particles. For this size range the following theoretical expression by

Knutson (1976), as an approximation to a more complicated expression formulated by Gentry (1972) provides a better fit to available data

$$\phi_v(d_p) = \begin{cases} \frac{1}{2+(0.1/d_p)^{1.5444}} \; ; \; if \; v = \pm 1 \\ 0 \qquad\qquad ; \; if \; |v| > 1 \end{cases} \qquad (2)$$

where d_p is in micrometers.

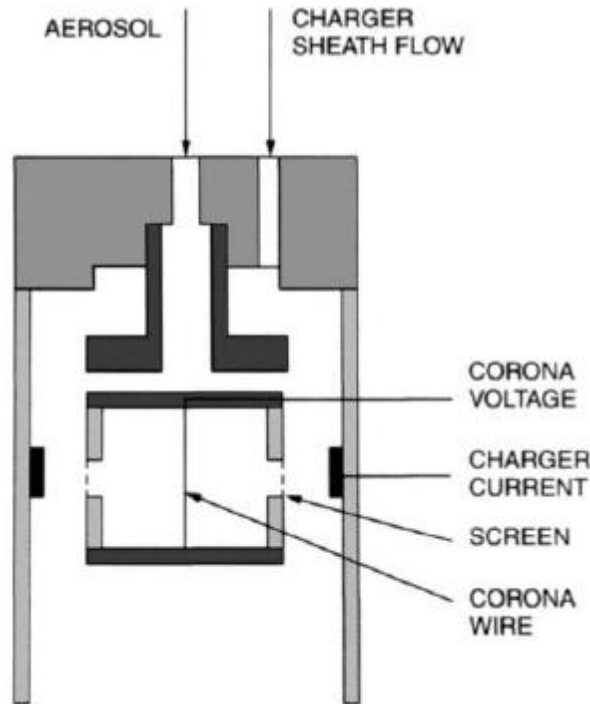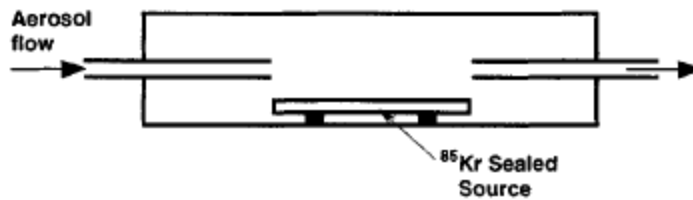**Figure 2. 5 Unipolar diffusion charger used in the TSI electrical aerosol analyzer**

Figure 2. 6 Bipolar diffusion charger based on a sealed ^{85}Kr β-particle source

2.2.2 Differential Mobility Analysis (DMA)

A DMA (Fig. 2.6) consists of a grounded outer cylinder and a concentric inner rod with a negative electrical potential. Two streams of air are introduced into the annulus region.

The smaller flow is the aerosol flow, q_a, is introduced from the outer cylinder. The sheath air flow, q_{sh}, consists of filtered air, and serves to carry the particles downstream the aerosol inlet. These two air streams flow side by side down through the DMA. Typically DMAs operate with a flow ratio $\frac{q_a}{q_{sh}} = 0.1$. Near the bottom of the DMA, the sample aerosol flow, q_s, is withdraw through a slit in the inner cylinder. The second exit flow, q_m, is the main exit airflow, which passes through a separate exit and is discarded. The positive charged aerosol particles are deflected inward towards the inner rod. Those particles traversing the annulus with the mobility that the DMA is adjusted to transmit, arrive at the inner cylinder at the location of the slit and become incorporated into q_s.
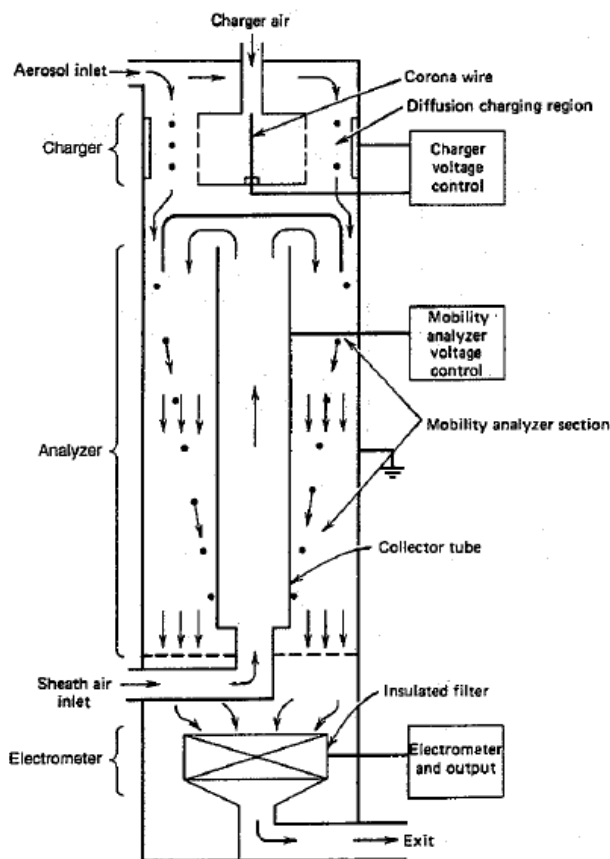
Figure 2. 7 Schematic diagram of a differential mobility analyzer (Adopted from Hinds, 1999).

2.2.2.1 Transfer Function and Resolution of DMAs

The ability of a DMA to classify aerosol particles having mobility $Z_p = \frac{qD}{kT}$, where q elementary charges and having diffusion coefficient D, can be described by its transfer function, i.e., the probability of a particle having electrical mobility Z_p, that enters the DMA to be included in the classification aerosol outlet flow (Knutson and Whitby, 1975).

In the first derivation of the DMA transfer function, Knutson and Whitby demonstrated that for non-diffusing particles this can be obtained without knowledge of the detailed structure of the flow field. Indeed, when assuming the particles are non-diffusing the only uncertainty in mobility classification can be entirely attributed to the finite stream width of aerosol flow.

In real conditions, the transfer function shape is closer to a Gaussian, with height less than unity and base width larger than $Zp_{max} - Zp_{min}$, as a result of particle diffusivity. Brownian motion of the charged particles makes the particles deviate from their deterministic trajectories, and as a result be included in the monodisperse particle outlet when they are not supposed to be included. The distorting effect of Brownian motion on the shape of the transfer function has been studied by a number of authors (Tammet, 1970; Kousaka et al., 1985, 1986; Stolzenburg, 1988; Rosell-Llompart et al., 1996; Stratmann *et al.*, 1997; Hagwood et al., 1999; Salm, 2000; de la Mora, 2002). Stolzenburg (1988) investigated the role of particle Brownian diffusion on the shape of DMA transfer function using an approach similar to that used by Tammet (1970) in his analysis of ion diffusion in aspiration condensers, and derived an expression of the transfer function of the cylindrical DMA. Recently, Salm (2000); Kulkarni and Wang (2006) proposed a different approach to account for broadening of transfer function due to particle Brownian diffusion.

Thus, DMAs with shorter column lengths and the ability to operate at high sheath flow rate are preferred for nanometer particles. The upper sizing limit a DMA can size/classify is determined by the maximum electrical strength achievable (i.e., the electrical breakdown voltage of the carrier gas). A long-column DMA is needed to extend the measurement range to sizes up to 1 micron. One of the tasks in particle mobility measurements is the estimation of the resolution. According to the DMA operation theory (Knutson and Whitby 1975; Stolzenburg 1998) the sizing resolution of a DMA is a function of the sheath-to-polydisperse-aerosol flow rate ratio. In a simple term, if polydisperse aerosol and monodisperse aerosol flow rates were kept constant, the better resolution would be achieved as the sheath flow rate is increased. The resolution parameter has also been expressed as $R = \frac{Z}{\Delta Z_{min}}$, where ΔZ_{min} is the least distinguishable interval in the spectrum at mobility Z (Salm, 1983; Zhang and Flagan, 1996). The interval ΔZ_{min} may be determined by means of the width of a normalized apparent spectrum (Salm, 2000). Moreover, Flagan (1999) described the resolution of the DMA as the ratio of the mobility

at the peak of the column of the transfer function to the full width of the transfer function at the one half of its maximum value.

The conditions that lead to diffusional broadening have been explained in a number of ways. Several reports have suggested that reducing the residence time of the particles in the classifier column is essential for high resolution measurements. While it is true that a short residence time reduces the extent of diffusion, diffusion is only important if the residence time is large by comparison to the characteristic time for the diffusion. Absolute residence time constraints do not necessarily eliminate diffusional broadening. de la Mora *et al*. (1998) at their paper have investigated ways to raise the resolution of DMAs. They concluded that the peak broadening may be reduced by two different means: the purely geometrical one, who involves using a DMA length comparable to its width, while the second approach involves augmenting the Peclét number, which may be achieved merely increasing the sheath flow rate.

Substantial progress has been made in improving the resolution of conventional instruments at the large particle end of the size spectrum. Through detailed numerical descriptions of the flow in the TSI long DMA, Chen and Pui (1997) have shown that a small classification voltage offset that has frequently been observed in tandem differential mobility measurements results from a recirculating flow within the entrance slot of the DMA. Refinements to the inlet slot design have eliminated this deviation and produced DMAs that are capable of operating with near-theoretical resolution at higher limiting resolutions that previously achieved (Chen et al., 1999; Eichler et al., 1998).On the other hand, the resolution of the Radial DMA (RDMA) was found to be somewhat lower than expected for large particles, but the high transmission efficiency for ultrafine aerosol particles has made it an extremely useful instrument for measurement of fine particle size distributions in clean atmosphere (Zhang et al., 1995).

2.2.3 Review of Aerosol Analyzers

2.2.3.1 DMAs

Differential mobility analyzers (DMAs) are widely used in aerosol research as a tool for sizing and for producing monodisperse airborne particles having diameters in the submicron and nanometer range (cf. Flagan, 1998; McMurry, 2000). In view of improving several aspects of their performance (e.g., particle size range, resolution etc.), several

DMA designs have been proposed over the last decades (Liu and Pui, 1974; Knutson and Whitby, 1975; Pourprix and Daval, 1990; Pourprix, 1994; Zhang *et al*., 1995; Zhang and Flagan, 1996; Fissan *et al*., 1996; Brunelli *et al.,* 2009; Santos *et al*., 2009). The most popular DMA design employs two coaxial cylindrical electrodes between which an annular flow carries the sample particles in a sheath particle-free flow (Whitby and Clark, 1966; Liu and Pui, 1974; Knutson and Whitby, 1975). Applying a potential difference between the two cylindrical electrodes, the charged particles migrate from one electrode to the other so that only particles having mobilities within a very narrow range can exit through the monodisperse exit. The DMA can be used except for the production of a monodisperse aerosol, for studying changes in aerosol particles due to condensation, evaporation, or other processes that will change the particle size or structure (McMurry, 2000).

Conventional DMAs employ one monodisperse-particle outlet. As a result, particles having mobilities only within a specific narrow range can be classified for each combination of operating conditions (i.e., flows and applied voltage between the two electrodes). This, however, poses the limitation that when DMAs are used as particle classifiers in aerosol-mobility spectrometers, it is required to scan through different operating conditions, thereby requiring a significant amount of time (from 30 seconds and up to a few minutes depending on the required accuracy of the measurement) for a single mobility distribution measurement (Wang and Flagan, 1990; Endo *et al.*, 1997).

In addition, because typically the flow field is usually kept constant and only the electric field is altered in order to classify particles of different mobility, the dynamic size range of conventional DMAs can span over one order of magnitude (McMurry, 2000). DMAs with multiple outlets on the other hand can significantly reduce the scanning time when used as classifiers in mobility spectrometers because particles of different mobility can be selected and detected simultaneously. Depending on the distance between the first and the last outlet from the inlet, one can also increase the dynamic mobility range of the selected particles in a single measurement.

Another limitation of the conventional cylindrical DMA is that classification of particles having diameter smaller than 10 nm is limited by the diffusivity of the particles along their migration paths. As a result, the transfer function of the instrument in this size region is broadened, and the classification resolution significantly reduced (Fissan *et al.*, 1996). To overcome this limitation Chen *et al.* (1998) proposed the use of shorter cylindrical DMA

columns to minimize the migration time of the particles within the instruments and thus to reduce the broadening of the transfer functions. To further improve the classification resolution of sub-10 nm particles, de la Mora and his co-workers have designed DMAs that operate at much higher sheath flow rates that can classify ions with sub-1 nm effective diameter (Rossel- Llompart *et al.*, 1996; de Juan and de la Mora, 1998; Ramiro *et al*., 2003).

In a multi-channel electrical mobility spectrometer, one of the electrodes is equipped with a series of insulated metal rings, each connected to its own electrometer. When a certain electric field is applied between the coaxial electrodes, the charged particles of a given polarity are deposited differentially onto the metal rings. This arrangement allows for the simultaneous measurement of the number concentration of particles having different mobilities, thus reducing considerably the time required for the measurement of the entire mobility distribution. The multi-channel analyzer, which has been specially designed for rapidly fluctuating aerosols, was developed in the 1970's at the University of Tartu (Tammet, 1970; Tammet *et al.*,1998, 2002). Other electrical mobility spectrometers that have been proposed in the past can measure particles having diameters over a wider range (e.g., Winklamayr *et al.*, 1991; Biskos *et al.*, 2005). Two commercial versions of DMAs of this design are the DMS, Differential Mobility Spectrometer, (Biskos *et al*., 2005) and the EEPS, Engine Exhaust Particle Sizer (TSI Model 3090). According to the specifications, the DMS is able to measure particles in the size range from 5 to 1000 nm with 26 channels, and the instrument response time is 500 ms. Similarly, the EEPS is capable of measuring aerosols in the size range from 5.6 to 560 nm in 22 channels, and its response time is 100 ms. The main disadvantage of these instruments, however, is that they do not have as good a size resolution as that provided by a conventional DMA.

Another approach to widen the classification size range of a DMA is that proposed by Seol *et al*. (2002) who designed and operated an adjustable-column length DMA (ACDMA) and showed that the classifier can measure particles having size from 1 nm to hundreds of nanometers by adjusting the column length, between 0 and 300 mm, corresponding to the particle size. Another way to expand the size range of the classified particles in one voltage scan is by varying the sheath flow rate as proposed by Collins *et al.* (2000). Operating the TSI model 3071 with the sheath flow rate ramp, i.e., 30-second ramp from 20 to 2 lpm, and voltage scanning, the lower particle size limit was decreased from

9.8 to 4.8 nm and the upper limit increased from 537 to 1160 nm. Further, Takenchi *et al.* (2005) proposed a dual-DMA design to measure particle in a wide size range. In the dual-DMA, the polydisperse aerosol flow is split into two streams, directed to two coaxially nested DMAs sharing the same electrically grounded cylinder. With two different sheath flow rates and classification lengths, the device, operated at the voltage ramp mode the researchers were able to separately monitor particles in the nucleation mode and accumulation modes of particulates emitted from diesel engines. The design essentially hybridizes two traditional DMA columns in one package. Additional to the two sheath flow controllers, two high voltage power supplies are needed in this device. Further, the generalization of this DMA design is limited if monodisperse particles of more than two different sizes were needed simultaneously. Note that the scanning time of this dual-type DMA is 2 min, the same as that of current SMPS. In an attempt to make a DMA that could scan faster through different channels, Chen *et al.* (2007) built and tested a classifier (MDMA) having three monodisperse-particle outlets. Each stage of MDMA column covers a fraction of the entire particle size range to be measured. The covered size fractions of two adjacent stages of the MDMA are designed somewhat overlapped. The arrangement leads to the reduction of scanning voltage range and thus the cycling time of the measurement. The performance of this DMA has only been determined experimentally, and to the best of my knowledge there is still lack of a theoretical model for predicting its behavior under different operating conditions.

During the last fifteen years, a great effort has been addressed to the improvement of the performance of DMAs, mainly modifying the aerosol inlet geometry in order to reduce diffusional deposition losses (Winklmayr *et al.*, 1991; Chen *et al.*, 1999), and shortening the mean aerosol residence time by minimizing the column length (Rosell-Llompart *et al.*, 1996) and operating the DMA in laminar flow conditions with sheath gas flow at high Reynolds for classifying ions with high resolution (Rosell *et al.* 1996; Eichler, 1998; de Juan and de la Mora 1998; Ramiro *et al.* 2003; Martinez-Lozano and de la Mora, 2006a). Also, two new conceptions of analyzers have appeared, one in which an additional electric field parallel to the main gas flow is applied (Loscertales, 1998), and the other type of DMA incorporating an electrified screen which permits maintaining the electrodes containing the inlet and outlet slits at the same potential (Martinez-Lozano *et al.*, 2006a,b), thus preventing electrophoretic losses. All the above mentioned improvements were implemented in concentric cylindrical DMAs. With this geometry, electrode centering is

critical to the performance of a DMA; even a very small misalignment of the electrodes can lead to a severe deterioration of the resolving power of the instrument. At the same time, Zhang and Wexler (2006) described a modern, miniaturized version of a multichannel parallel-plate DMA suitable for analyzing gas phase compounds or volatile particle phase compounds. In these DMAs the electrodes were rectangular planar plates.

2.2.3.2 Tandem-DMAs

The differential mobility analyzer (DMA) (Hewitt, 1957) has been widely applied in a variety of aerosol measurement applications including the generation of monodisperse aerosol standards for instrument calibration (Liu and Pui, 1974) and the measurement of submicron aerosol size distributions (Knutson, 1976; Hoppel, 1978; Fissan *et al*., 1982; Plomp *et al*., 1982; Scheibel *et al*., 1983; Kousaka *et al*., 1985). The use of two or more DMAs in series, referred to as a tandem differential mobility analyzer (TDMA) system, has, also, been made to probe intrinsic particle properties. The TDMA technique can be used for measuring the difference broadening of the DMA transfer function. Rader and McMurry (1986) demonstrated that the TDMA technique is extremely sensitive, as they measured diameter changes with a precision of about 0.3%. Moreover, Kousaka *et al*., (1985) confirmed that for ultrafine particles diffusion within the DMAs leads to major discrepancies between the TDMA measurements and theoretical predictions of size distributions based on the theory of Knutson and Whitby (1975).

TDMA measurements have been made for studying deliquescent and hygroscopic properties of monodisperse aerosols (Liu *et al*., 1978), for the reaction rate between ammonia gas and sulfuric acid aerosol droplets (McMurry *et al*., 1983) and for evaporation rates of several organic aerosol materials (Rader *et al*., 1986b). A TDMA system typically consists of five components (cf. Fig. 2.7):

    a. a DMA

    b. an aerosol conditioner

    c. a measuring DMA, and

    d. an aerosol detecting subsystem.

Monodisperse aerosol particles generated by DMA-1 undergo a size change in the aerosol conditioner before entering DMA-2. Size changes occur, for example, as a result of particle evaporation, condensation of gaseous species onto the particles, and/or heterogeneous

chemical reactions are allowed to occur in the conditioner. In consequence, DMA-2 is used to measure the change in particle size that occurs in the aerosol conditioner.
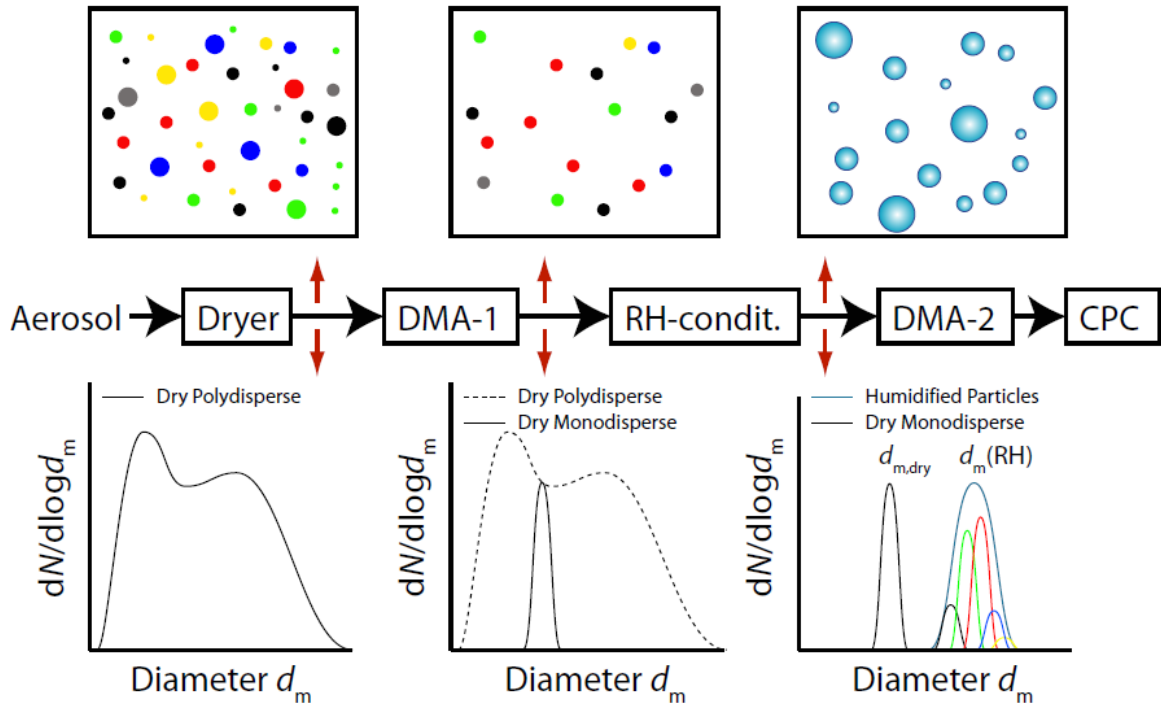
Figure 2. 8. Tandem Differential Mobility Analyzer (TDMA) operation

2.3 Instrument Response

2.3.1 DMA Response

The DMA has been used for measuring size distributions of aerosols (eg. Knutson 1976; Hoppel, 1978; Alofs and Balakumar, 1982; ten Brink *et al*., 1983). Also, Rader and McMurry (1986) have reported the tandem DMA (TDMA) measurement technique, for the cases of measuring growth or evaporation rates of monodisperse aerosols. While the above mention applications used the non-diffusing transfer theory, Stolzenburg (1998) take into account the diffusion effects on the measurement problems. The concentration and the size distribution of the aerosol particles exiting the DMA depend on both operating characteristics of the DMA, and on characteristics of the aerosol sample. The diameter and charge distribution of the classified aerosol are defined as $n(d_p, n_p)\mathrm{d}d_p \equiv$ number of particles per unit volume entering the classifier with charge n_p and diameter in the range d_p and $d_p + \mathrm{d}d_p$, and $\hat{n}(Z_p)\mathrm{d}Z_p \equiv$ number of particles per unit volume entering the classifier with electrical mobility in the range Z_p and $Z_p + \mathrm{d}Z_p$, respectively (Stolzenburg, 1988). Thus, in combination with the DMA transfer function, Ω, (eg. Stolzenburg (1988),

Eq. 2.69) the mobility distribution exiting the DMA is given by the relation: $\frac{q_a}{q_s}\Omega(\tilde{Z}_p)\,\hat{n}(Z_p)\mathrm{d}Z_p$, where $\tilde{Z}_p$ is the dimensionless electrical mobility, which equals to the number of particles per unit volume exiting the classifier with electric mobility in the range Z_p and $Z_p + \mathrm{d}Z_p$. We note that $\hat{n}(\tilde{Z}_p)$ can be reduced to a size distribution function multiplied by various size dependent factors characterizing the aerosol system upstream of the classifier, e.g. fraction charged, transport efficiency.

In most cases $\Omega(\tilde{Z}_p)$ is a much narrower function than $g(\tilde{Z}_p) \equiv \frac{q_a}{q_s}\,\hat{n}(Z_p)$ such that the behavior of the output distribution is dominated by characteristics of the classifier transfer function. Thus, effects of the shape of the input distribution on the output distribution can be treated as perturbations of this basic behavior. For example, if we consider the base case of a flat input distribution, i.e. $g(\tilde{Z}_p) = g\,(constant)$, then the output distribution, i.e., $g\Omega(\tilde{Z}_p)$ is a scaled form of the transfer function.

The classification system includes, a measuring subsystem, e.g. condensation particle counter (CPC), aerosol electrometer (AE), optical particle counter (OPC), which produces a measurable response that is proportional to aerosol number concentration. A response function can be defined for the measuring subsystem as: $R(d_p, n_p) \equiv$ response of receiving subsystem (sensor) per unit concentration of particles received of charge n_p and diameter d_p.

Thus, what is, typically, measured in such a DMA measurement system (Fig. 2.8) is the integrated response of the measuring subsystem given by (Stolzenburg, 1988):

$$I(V) \equiv \int_0^\infty R(d_p, n_p)\,\frac{q_a}{q_s}\Omega(\tilde{Z}_p, n_p, V)\,n(d_p, n_p)\mathrm{d}d_p \qquad (3)$$

as a function of the voltage applied to the central rod, $V < 0$.

Let $R(V)$ denote the response of the sensor as a function of the rod voltage, for a CNC, the response has units of cm^{-3}, while for a current meter type sensor has units of amperes. For an CNC, the response to a single particle is independent of the number of charges on it, while for the electrometer the response is weighted more heavily towards the multiply charged particles.

The factor relating sensor response to the flux (particles/sec) of the particles is equal to:

$$W_v = \frac{v}{6.24 \times 10^{18}} \left(\frac{Asec}{electron}\right) \text{ , and} \tag{4a}$$

$$W_v = \frac{1}{q_s} cm^{-3} \tag{4b}$$

for the current meter and the CNC, respectively, where v is the number or elementary charges (Alofs and Balakumar, 1982).

Thus, Eq. (3) can be written to its equivalent form:

$$I(V) \equiv q_a \sum_{v=1}^{\infty} W_v \int_0^{\infty} \phi_v(d_p)\Omega(\tilde{Z}_p, n_p, V)\, n(d_p, n_p)\, \mathrm{d}d_p \tag{5}$$
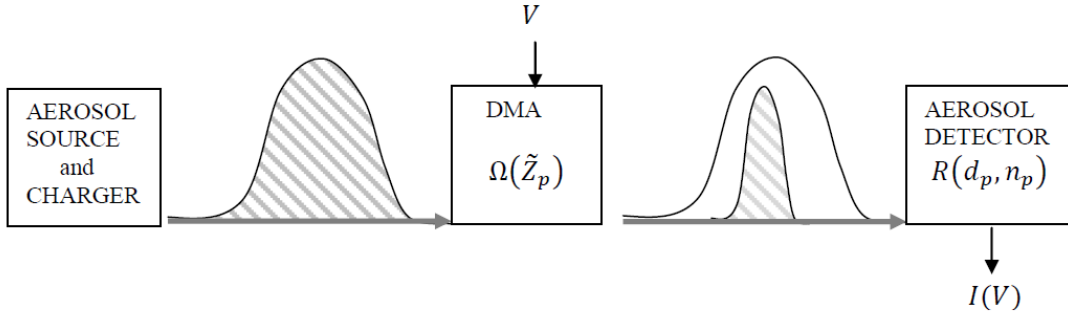
Figure 2. 9 DMA Aerosol Measurement System

2.3.1 TDMA Response

The aerosol introduced at the TDMA system (Fig.2.7) is characterized by the mobility distribution, $\hat{n}(Z_{p1})$, Then, DMA-1 extracts a nearly monodisperse segment about the centroid mobility Z_{p1}^* according to the transfer function $\Omega_1(Z_{p1}, V_1)$. The size of the particles exiting DMA-1 is changed, e.g. by condensation/evaporation, in the aerosol conditioner that has a penetration efficiency $P(Z_{p1})$, and transform the mobility of the particles according to the function $Z_{p2} = f_c(Z_{p1})$. Then, the conditioned aerosol is reclassified in DMA-2 according to the transfer function $\Omega_2(Z_{p2}, V_2)$ having centroid mobility Z_{p2}^*. Finally the aerosol concentration exiting the second DMA is determined by the sensor with response function $R(Z_{p2})$. Consequently, the signal produced by the TDMA system is the integrated responses of the aerosol detector as a function of the DMAs voltage settings, i.e.

$$I(V_1, V_2) \equiv \int_0^{\infty} R(Z_{p2}) \frac{q_{a2}}{q_{s2}} \Omega_2(Z_{p2}, V_2) P(Z_{p1}) \frac{q_{a1}}{q_{s1}} \Omega_1(Z_{p1}, V_1)\hat{n}(Z_{p1}) \mathrm{d}Z_{p1} . \tag{4}$$

2.4 Aerosol Measurements Data Inversion

2.4.1 Inversion: The Basic Mathematical Problem

Physical theories allow us to make predictions: given a complete description of a physical system, we can predict the outcome of some measurements. This problem of predicting the result of measurements is called the modelization problem, the simulation problem, or the forward problem. The inverse problem consists of finding an unknown property of an object from the actual result of some measurements of this object to a probing signal (Tarantola, 2005; Ramm, 2005).

For aerosol size spectrometers instrument response is analogous to the size distribution being measured. The data inversion problem then amounts to determining which distribution caused a given measured response in an instrument the linear response curve of which is known. In general, a finite number of instrument responses is obtain, so that the problem can be declared as (Crump and Seinfeld, 1982):

Find the size distribution f such that

$$L_i f = y_i, \qquad i = 1,2,\dots,n, \tag{5}$$

where f is the unknown size distribution, y_i the ith datum, and L_i the ith instrument response linear functional. Problem (5) is called well posed if it is uniquely solvable for every y and the solution f varies continuously with the data y. A well-posed problem is characterized by the following three conditions (Crump and Seinfeld, 1982):

  a. For every y there is a solution f.
  b. The solution f is unique.
  c. The solution f is stable.

The solution f is called stable if, for any sequence of perturbations in y tending to zero, the corresponding sequence of perturbations in the solution f also tends to zero. If the condition a. fails the problem is overconstrained and if condition b. fails is underdetermined. Even if a-c hold for the system of problem (5), it may happen that small perturbations in the data y cause relatively large disturbances in the solution f, then the problem is called ill-conditioned, i.e., that makes clear an extreme insensitivity of the data to large perturbations in the solutions.

In general, the linear functionals L_i are linear integral operators of the Fredholm type, that is, $L_i f = \int K_i(x) f(x) dx$. As, almost any function that oscillates rabidly enough can

be added to a solution of Eq. 5, without affecting it's validity, it can be concluded that Eq. (5) itself is not sufficient to afford solution of the inversion problem, but some additional information will be needed to be used in order to obtain acceptable solutions. The above mentioned points are general characteristic of ill-posed problems. Tikhonov and Arsenin (1977) investigate such problems and states what criteria should be used for their solution.

Inversion problems arise repeatedly in the determination of aerosol size distribution, as a particular channel of the aerosol spectrometer will collect particles from multiple size ranges. A degree of indeterminacy is introduced into the measurements, so that a continuous size distribution has to be estimated from a set of discrete measurements, each of which is influenced by all values of the unknown distribution, i.e. the distribution function must be found, as it were, from a tangled set of combinations of measurements (Twomey, 1977).

In the case of aerosol size distribution measurements with a mobility analyzer the general inversion problem (Eq. 5) can be written as:

$$y_i = \int_a^b K_i(x)f(x)dx + \varepsilon_i, \quad i = 1,2,\dots,N \tag{6}$$

where y_i are the discrete measurements points, $f(x)$ the unknown size distribution function, x is a size parameter, K_i is the kernel function of the ith instrument channel (i.e. the instrument response), a and b are the size limits within which the size distribution lies, and ε_i is the instrument error in that channel.

Equation 6, the Fredholm integral equation of the first kind, can be approximated by a sum using numerical quadrature so that

$$\begin{aligned} y_1 &\approx \sum_{j=1}^m A_1(x_j)f(x_j) + \varepsilon_1, \\ y_2 &\approx \sum_{j=1}^m A_2(x_j)f(x_j) + \varepsilon_2, \\ &\vdots \\ y_N &\approx \sum_{j=1}^m A_N(x_j)f(x_j) + \varepsilon_N \end{aligned} \tag{7}$$

where the interval [a, b] has been divided into m subintervals, and $A_i(x_j) = K_i(x_j)\Delta x_j$. Consequently, we have a system of N equations in m unknowns, the unknowns being the values of f at the midpoints of the m subintervals. Eq. 7 is a set of linear equations but routine techniques for solving systems of linear equations cannot be applied on this problem. The equations in Eq. 7 are merely approximate not only because of the finite

error in representing an integral as a discrete sum but also because of the errors in measurement.

An equivalent form of Eq. 7, in matrix notation, is $y = Af + e$, where y and e are $N \times 1$ vectors, f is a $m \times 1$ vector, and A is a $N \times m$ matrix. A simple matrix inversion (ignoring the error terms) will lead to an estimate of f, i.e. $\hat{f} = A^{-1}y$. But, for a straightforward inversion procedure to be applied, the linear equations must be independent of each other. If any subsets of equations in Eq. 7 are dependent on one another, i.e. one equation can be expressed as a linear combination of the other equations, then the matrix A becomes singular and the inverse does not exist. For many indirect measurements encountered in aerosol science and elsewhere, the equations are "quasi-dependent" on each other, so that the matrix is "nearly" singular and A^{-1} becomes very large. This quasi-dependency arises due to the large degree of overlap between the kernels over the region of interest. This overlap reflects the fact that particles of a certain size can be counted on more than one channels. Then each additional measurement contains progressively less new information and therefore is, to some extent, redundant.

As pointed out from Twomey (1977) and Kandlikar and Ramachandran (1999) in function space, the measurements of $\int_a^b K_i(x)f(x)dx$ can be treated as the projections of the unknown $f(x)$ on the set of axes $K_1(x)$, $K_2(x)$, etc. If the kernels $K_1(x)$, $K_2(x)$, etc were completely independent of each other, they would be mutually orthogonal. However, since they are not completely independent, the axes formed by them are skewed (Figs. 2.9 a and b, adapted from Twomey, 1977) show a simplified representation of this situation with only two such axes, $K_1(x)$, $K_2(x)$.
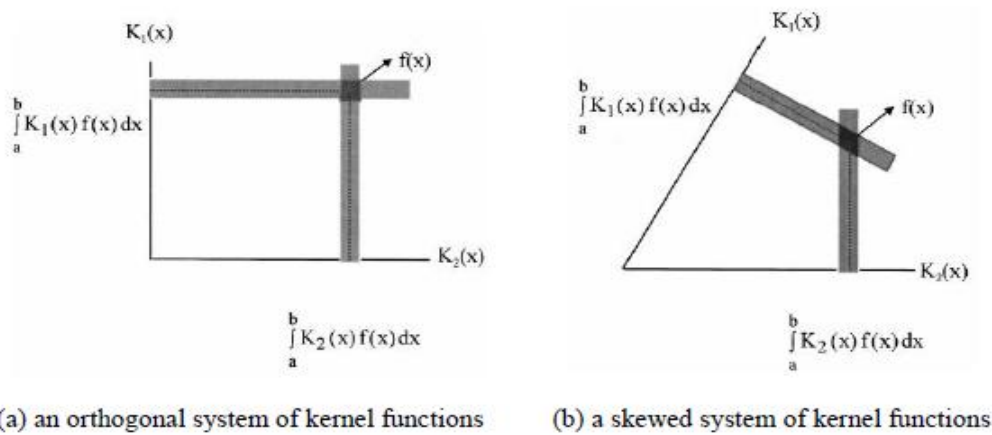
(a) an orthogonal system of kernel functions (b) a skewed system of kernel functions

Figure 2. 10 Effects on errors on (a) an orthogonal system of kernel functions, (b) a skewed system of kernel functions (adapted from Twomey, 1977)

The orthogonality of the axes becomes important due to the measurement error. If there is some measurement error, e.g. shaded region in Fig. 2.10(a), then it translates into an uncertainty in the solution $f(x)$, indicated by the darker area. However, if the axes are not orthogonal as in Fig. 2.10(b) then the same amount of measurement uncertainty leads to a much larger solution uncertainty. The error in the solution is given by the relation $f - \hat{f} = A^{-1}y - A^{-1}(y - e) = A^{-1}e$. It indicates, as already mentioned, that the solution is unstable in that a small error in measurement can lead to a very large error in solution due to the large values of A^{-1}, and thus, results to a 'ill-posed' problem.

The skewness in the axes can be overcome by orthogonalising the kernels $K_i(x)$ using the Gram-Schmidt procedure (Twomey, 1977) or some other procedure so that the solution $f(x)$ can be represented as a sum of orthogonal functions. If $\lambda_1, \lambda_2, ..., \lambda_N$ are the eigenvalues of A then, A is singular if at least one eigenvalue is equal to zero, while is near-singular in the case that some eigenvalues are very close to zero. Then the solution can be written as $\hat{f} = A^{-1}y = \sum_{i=1}^{N} \lambda_i^{-1} c_i u_i$, where u_i are the orthogonal eigenvectors of A, c_i are coefficients of the eigenvectors. As, the reciprocals of the small eigenvalues are very large, and if there are any errors in the measurements, y, these errors will be extremely magnified by these reciprocal eigenvalues, so that the solution f will have a very large error in it. Thus, orthogonalisation by itself also does not solve the problem of ill-posedness. In fact, the small eigenvalues of A just reflect the high degree of interdependence among the kernel functions.

Another problem to be taken into account in finding the size distribution measurement is that in most applications in aerosol science, the system of equations in Eq.7 is underdetermined with the number of measurements less than the number of unknowns, i.e. $N < m$. Thus, even in the absence of measurement error, there is no unique solution. Many solutions satisfy the same set of measurements. Thus, there is not enough information to solve the problem uniquely. In order to select one among a multitude of solutions, additional information has to be added to the system. This is done in the form of *a priori* constraints on the solution. To some extent, these constraints are arbitrarily imposed, and hence care should be taken to ensure that the constraints are physically justifiable.

In the following sections, we will describe a selection of techniques that siege to give solution to this problem in different ways with differing levels of success. The methods include linear approaches such as least-squares solutions, regularisation, and decomposition techniques that use basis functions, non-linear approaches that use gradient search methods, extreme value estimation, and Bayesian methods. In general, any technique that proposes to solve an ill-posed problem will have to provide a scheme by which

  a. one among a multitude of possible solutions is selected as "the solution",
  b. error magnification is minimized, and
  c. the chosen solution provides a good fit to the data.

2.4.2 Aerosol Data Inversion Techniques

Several different techniques are in use for reconstructing aerosol size distributions from experimental data. Each of these techniques has certain deficiencies, and indeed, it is doubtful that any method can fulfill the ideal of perfect reconstruction of a size distribution from a limited set of data. A list of inversion methods used in aerosol size measurements is presented in Table 2.1.

Knutson (1976) published the first method for inverting the data from a DMA (with a bipolar charger upstream) to obtain aerosol size measurements. The Knutson method required various approximations and assumptions which he did not numerically justify in his paper. However, the Knutson inversion technique is extremely simple, in that it yields a system of linear equations which may be solved recursively.

The second inversion algorithm to be published for the Electrical mobility analyzer was given by Hoppel (1978). It consists of a successive approximation, in which the first approximation to the size distribution is obtained by neglecting the multiply charged particles. The first approximation is then used to estimate the number of multiply charged particles, and thus obtain a second approximation. The process then repeats until it converges. Hoppel provided only a few numerical examples of the accuracy of his technique.

A third inversion technique was published by Haaf (1980). It consists of a trial and error procedure in which the response of the Electrical mobility spectrometeris calculated for an assumed size distribution, and compared to the actual measured response. The assumed size distribution is then adjusted until the difference between the actual response and the computed response is a minimum. The inversion method proposed by Haaf is much more complicated than that by Knutson or that by Hoppel, and yet in a sense is more familiar in that such a procedure is usually required when inverting indirect measurements. Twomey (1975) applied a similar iterative procedure to inverting filter transmission measurements to obtain aerosol size distributions.

2.4.2.1 Linear Methods

2.4.2.1.1 Least-squares solution

One approach to providing additional information is to overdetermine the problem by making the number of unknowns less that the number of measurements. This could be achieved by representing the unknown distribution parametrically, e.g. as a bimodal lognormal distribution. In such cases one seeks a "least-square" solution that minimizes the residual $(Af - y)^T(Af - y)$, which leads to the solution $f_{l-s} = (A^T A)^{-1} A^T y = A^+ y$. But, as the elements of A^+ remains large, they lead to "catastrophic error amplification" (Enting and Newsam, 1990). The error in this case, can be calculated as $f_{l-s} - \hat{f}_{l-s} = (A^T A)^{-1} A^T y - (A^T A)^{-1} A^T (y - e) = A^{-1} e$. Moreover, the initial guess solution for the minimization procedure often determines the final solution, and thus the least-squares approaches do not provide any benefit in solving ill-posed problems. Gonda (1984) notes that assuming a parametric form for the unknown distribution easily provides a unique solution where convergence is achieved by user intervention between successive iterations.

2.4.2.1.2 Constrained least-squares

First Phillips (1962) and later Twomey (1963) proposed a constrained least-square approach, in which additional information in the form a smoothness constraint is added

whereby the chosen solution is the smoothest possible while still restricting the error residuals to be within reasonable bounds. The second difference expression $\sum_{j=1}^{m}(f_{j-1} - 2f_j + f_{j+1})^2$ was used as a measure of smoothness, so that the smoothest solution was one that minimized it. Even though, the minimization of the second-differences expression has become the most commonly employed smoothness criterion, it may not always be the most appropriate. Thus, if a solution has several sharp peaks, the second-differences criterion might eliminate them altogether; in such cases, a first-difference measure such as $\sum_{j=1}^{m}(f_{j-1} - f_j)^2$ of $\sum_{j=1}^{m}(f_j)^2$ or the deviation from a trial solution p_j, i.e., $\sum_{j=1}^{m}(f_j - p_j)^2$ can be used. Regardless the smoothness criterion the problem can be framed as the minimization of $f^T H f$ while holding $(Af - y)^T(Af - y)$ constant, i.e. the minimization of $(Af - y)^T(Af - y) + \gamma f^T H f$, which yields the Twomey-Phillips solution $\hat{f}_{T-P} = (A^T A + \gamma H)^{-1} A^T y$, where H matrix is nearly diagonal and depends on the smoothing constraint of choice.

Twomey (1977) gives the H matrix for a number of different constraints. If γ is chosen equal to zero, this is equivalent to inverting a near-singular matrix with some very small eigenvalues. As γ is increased, the smallest eigenvalues are filtered out, and information is added to the system which uniquely selects a solution. Rizzi et al. (1982) used this approach to retrieve aerosol size spectra from simulated spectral optical depths in the wavelength range from 0.37 to 2.2 μm. Small values of γ between 10^{-4} and 0.05 provide the best solutions where information on the shape of the true solution is retained even if the retrieved solution is not well-behaved (i.e. the solution may take on negative values, and therefore is non-physical). Higher values of γ yield well-behaved solutions; however, in such cases the first-guess solution has a strong effect on the final solution. They also determined that the techniques tolerated a maximum error of 5% in the measurements before the retrievals were severely degraded. Cooper and Spielman (1976) proposed that instead of suppressing ill-conditioning by smoothing, one should impose only physical constraints on the solution, e.g. that the solution be non-negative and the area under the solution curve be unity. However, as Lesnic *et al.* (1995) showed this is not enough by itself to reduce ill-posedness and we need both physical constraints and smoothness constraints.

2.4.2.1.3 Tikhonov regularisation

A regularisation method is a method of overcoming ill-posedness by replacing the problem with a 'nearby' well-posed problem whose solution approximates the required actual solution, but which is more satisfying than that obtained by simple least-squares regression. Two additional pieces of information are supplied by the analyst: a smoothness ctiteria J, and a regularisation parameter, λ, which controls the degree of smoothing that is applied, and hence the level of filtering to eliminate noise in the solution. The best known regularisation method is that of Tikhonov and Arsenin (1977), which finds a solution to the

minimization problem $\sum_{i=1}^{N}\left[\frac{y_i - \int_a^b K_i(x)f(x)dx}{E(e_i)}\right] + \lambda J = R(\lambda) + \lambda J(\lambda),$ (8)

where the first term, R, is a residual that measures the agreement of a solution with measured data while the term J is a regularizing term, and λ is the regularisation parameter and $E(e_i)$ is the expected value of the error in the *ith* measurement. R and J are functions of λ, since the choice of the regularization parameter determines the degree of smoothing and the agreement with measurements.

Following Hansen (1992) and Hansen and O'Leary (1993), $J(\lambda)$ can be set equal to:

a) the norm of the unknown function itself, i.e. $J = \int_a^b (f(x))^2 dx$

b) the norm of the derivative or second derivative, i.e. $J = \int_a^b (f''(x))^2 dx$

c) the Shannon-Jaynes entropy, as the maximum entropy method calls (Shannon and Weaver, 1962) $J = \int_a^b f(x)\log(f(x))dx.$

As the choices (a) and (b) for J do not quarantee the non-negativity of the recovered size distribution a separate constraint of non-negativity has to be imposed. However, choice (c) provided an intrinsically positive size distribution. Yee (1989) used this approach to reconstruct size distributions from noisy diffusion battery measurements, and found that the method could even retrieve size distributions that were very sharp, i.e. Dirac delta functions.

These optimization methods can be viewed as minimizing J subject to keeping the size of the residual less than some fixed value, or conversely minimizing the residual subject to keeping J less than some fixed value. Lesnic *et al.* (1995) used the minimization of the norm of the first derivative subject to the constraints that R be less than some prescribed quantity, and the size distribution be non-negative.

For selecting the proper value for λ a number of approaches have been suggested:

a) *Zeroth-order regularisation.* This approach provides a solution that matches the measurements to just within expected experimental error. For example, Ramachandran *et al.* (1996) used this approach for handling personal cascade Impactor data by setting $\sum_{i=1}^{N} \left[\frac{y_i - \int_a^b K_i(x)f(x)dx}{E(e_i)} \right]^2 = N$, where N is the number of measurements.

b) *Generalised cross-validation (GCV).* A method proposed by Wabba (1977) and Golub *et al.* (1979) and used for aerosol inversion problems by Crump and Seinfeld (1982). When the approach of GCV is used if any measurement y_i is left out and a solution $f(x, \lambda)$ is calculated by minimizing Eq. 8, then $\int_a^b K_i(x)f(x, \hat{\lambda})dx$ should be closer to y_i than for other values of λ. As a measure of closeness can be used a data prediction error function, i.e. $V(\lambda) = \frac{1}{N}\sum_{i=1}^{N} \left[\int_a^b K_i(x)f(x, \lambda)dx - y_i \right]^2 w_i(\lambda)$, where the weights $w_i(\lambda)$ are chosen so that $V(\lambda)$ has the same minimizing value of λ as the mean square true prediction error $\frac{1}{N}\sum_{i=1}^{N} \left[\int_a^b K_i(x)f(x, \hat{\lambda})dx - \int_a^b K_i(x)f(x)dx \right]^2$, where $f(x, \hat{\lambda})$ is the solution minimizing Eq. 8 and $f(x)$ is the true solution (Wabba, 1977). Hansen and O'Leary (1993) stated that the disadvantage of this approach is that the GCV function can have a flat minimum and thus it may be difficult to be located numerically. Hence, they proposed the *L-curve* method.

c) *L-curve method.* The L-curve is a plot of $R(\lambda)$ vs $J(\lambda)$, as they are defined in Eq.8. $R(\lambda)$ measures the agreement of a solution with measured data, thus when $R(\lambda)$ is alone minimized, the agreement of solution with data becomes implausibly good, but the solution becomes unstable. $J(\lambda)$ is a stabilizing functional and is a measure of smoothness of the solution independent of the actual data. Figure 2.10 shows the trade-off between $R(\lambda)$ and $J(\lambda)$, which produces an empirically observed L-shaped curve. For small values of λ, the curve is almost vertical and solutions are unstable because they depend almost entirely on a close match with data so that experimental errors are amplified in the solutions. For large values of λ, the curve is flat and solutions are over-smoothed such that while the effects of measurement errors are filtered out, there is also some addition of constraint-generated information. Optimum

solutions lie near the corner of the L-curve. In this region, the solution strikes a balance between smoothness and fidelity to measurements. Lloyd et al. (1997a) use the L-curve method for analyzing diffusion battery data, and show that the solutions obtained are superior to those obtained by using the discrepancy principle. If the discrepancy principle is used, the results are dependent on the estimate of experimental error, whereas the L-curve method yields results that are independent of experimental error. A potential drawback to the L-curve method is that it is not convergent when the solution is "rough" (Vogel, 1996), i.e. the size distribution has a lot of peaks and valleys. Hansen (1992) shows that the L-curve criterion is similar to GCV and the discrepancy principle and whenever GCV finds a good value of λ, so does the L-curve method. However, the L-curve has several advantages over GCV: calculation of the corner of the L-curve is a standard numerical problem, and the method is quite able to handle correlated measurement errors which GCV cannot.
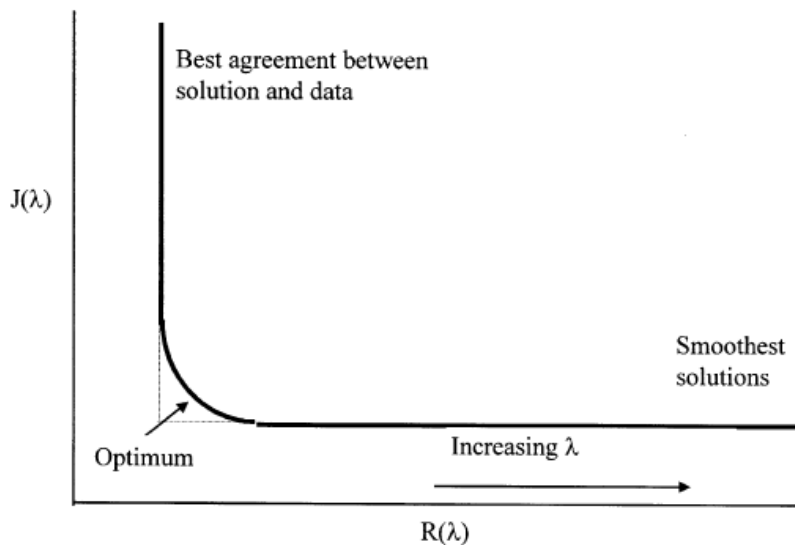
Figure 2. 11 The L-curve showing the trade-off between smoothness of solution and agreement of solution with measurements (adopted from Kandlikar and Ramachandran, 1999).

2.4.2.2 Non-Linear Iterative Methods

In this class of methods, a good initial solution, $f^{(0)}$, usually an educated guess, is refined repeatedly by multiplying the solution by correction factors $c^{(1)}, c^{(2)}, \dots, c^{(n)}$ so that the final solution is given iteratively by $f^{(n)}(x) = c^{(n)} f^{(n-1)}(x)$, where n is the iteration number.

2.4.2.2.1 The Chahine (1968) method

Chahine (1968) proposed a method firstly used for obtaining atmospheric temperature profiles and later for obtaining particle size distributions from light extinction measurements (Grassl, 1971), light scattering measurements (Santer and Herman, 1983) and for analyzing distributions of fractal objects from light scattering (Ferri *et al.*, 1989). In this method, an initial solution, $f^{(0)}$, is chosen such that it is always positive. The calculated measurements, $\int_a^b K_i(x)f^{(0)}(x)dx$, are compared with the actual measurements y_i, and adjustments are made to $f^{(n)}(x)$ in successive iterations so as to minimize each of the residuals, $\left[\int_a^b K_i(x)f^{(n)}(x)dx - y_i\right]^2$. In the Chahine algorithm the largest change in $\int_a^b K_i(x)f^{(n)}(x)dx$ can be caused by the least perturbation to $f^{(n)}(x)$ if the perturbation occurs at the point where $K_i(x)$ attains its maximum.

2.4.2.2.2 The Twomey (1975) method and modifications to it

Twomey's method (1975) overcome the problem of unrealistic, high-frequency oscillations in the Chahine solution, while retaining the positively constrained solutions and having no limitation on the number of points at which the solution is corrected. An initial guess solution is iteratively multiplied by small multiples of the kernel functions which are proportional to the ratio of the actual to calculated measurements, i.e.

$$f^{(n+1)}(x_j) = \left[1 + a_i^{(n)}K_i(x_j)\right]f^{(n)}(x_j), i = 1,2,\dots,N,$$

where $a_i^{(n)} = \left(\dfrac{y_i}{\sum_{j=1}^m K_i(x_j)f^{(n)}(x_j)\Delta x_j} - 1\right)$. In each iteration, a total of $m \times N$ corrections are made, as $f^{(n+1)}(x_j)$ is calculated for all x_j ($j = m$ values) for each of the measurements ($i = N$ values). If relative smooth kernels and relative small values of $a_i^{(n)}$ are assumed, then $f^{(n+1)}(x_j)$ is written as:

$$f^{(n+1)}(x_j) = \left[1 + a_1^{(n)}K_1(x_j)\right]\left[1 + a_2^{(n)}K_2(x_j)\right]\dots\left[1 + a_N^{(n)}K_N(x_j)\right]f^{(n)}(x_j).$$

This approach was used by Hitzenberger and Rizzi (1986) to retrieve size distributions from measured extinction coefficients at multiple wavelengths. Since the solution is a linear combination of the kernel functions, the high-frequency oscillations of the Chahine algorithm can be avoided. However, if the kernel functions themselves are not smooth or are oscillatory (e.g. in light scattering), these patterns will be seen in the solutions as well. Moreover, we cannot always neglect higher-order terms so that we may have terms

involving products of kernel functions in the solution. These product terms will magnify any oscillations in the kernels and cause large, artificial oscillations in the solution.

Markowski (1987) used a smooth initial guess for the Twomey algorithm. The output solution was then smoothened further by replacing each value $f(x_j)$ with the weighted average of all points in the neighbourhood: $f(x_{j-1})$, $f(x_j)$, and $f(x_{j+1})$. The smoothing is continued until the calculated measurements using the smoothed solution and actual measurements differ from each other sufficiently, when the solution is used as an input to the Twomey algorithm for iteration. This procedure is repeated until the solution is sufficiently smooth (as measured by the average absolute value of the second derivative of the solution). Thus, the modified Twomey method again seeks a compromise between agreement of the solution with the data and an arbitrary constraint (smoothness of the solution). This approach has been used widely in the aerosol field, most recently to obtain size distributions from measurements of spectral time-dependent radiation when aerosol particles are heated up using a laser and allowed to cool down by molecular heat conduction (Roth and Filippov, 1996).

An alternative modification of Twomey's method is that proposed by Winklmayr *et al.* (1990). Instead of smoothing the solution *post-facto*, they smooth the kernel functions in the Twomey algorithm beforehand, i.e. instead of using the actual kernel functions, $K_i(x)$, they use $(K_i(x)/max\ K_i(x))^r$, where the exponent r ranges between 0.3 and 0.7. They also use a very smooth initial guess solution, and use a chi-square statistic,

$\frac{1}{N}\sum_{i=1}^{N}\left[\frac{\int_a^b K_i(x)f(x)dx-y_i}{E(e_i)}\right]^2$, as a stopping criterion for the iterations.

2.4.2.3 Extreme Value Estimation

The extreme value estimation (EVE) method proposes that the set, D, of all solutions that produce a "well enough" fit is considered the solution (Paatero, 1991). A likelihood function $L(y/f)$ gives the probability or likelihood of a possible f being the cause of the measurements y. Best-fit methods try to maximise the likelihood function. If the error (ε) on y is normally distributed with zero mean and variance σ_y, then maximizing the likelihood function is equivalent to minimizing the least-squares term given by $Q(f_{l-s}) =$

$\sum_{i=1}^{N}\left[\frac{y_i-\int_a^b K_i(x)f(x)dx}{E(\varepsilon_i)}\right]^2$. Thus, the solution $f \in D$ if $D(f) < Q(f_{l-s}) + \Delta Q$, where the quantity ΔQ is a user-specified parameter, and determines the size of the set D, i.e. larger

ΔQ more values of f will be included in D. As the entire set D is of limited practical value, a scalar functional as $F = \sum_{j=1}^{m} c_j f_j$ is estimated, by forming a confidence interval $[F_{min}, F_{max}]$. Even though the idea of a set of acceptable solutions is more attractive than one prescribed best solution, in practice this technique is not much different from the least-squares approach with some relaxation of the best-fit criterion. Maximizing the functional F is akin to maximizing the norm of the unknown size distribution.

2.4.2.4 Bayesian Methods

Another class of techniques that solve inverse problems through statistical analyses of repeated solutions of the forward problem was introduced by Ramachandran and Kandlikar (1996). Bayesian statistics requires analysts to make explicit prior probabilistic judgments on physical parameters. From a Bayesian perspective, a measurement serves to refine previous knowledge of parameters by modifying these prior probability distributions. The process of refining previous knowledge of the parameters is also called updating and invokes the classic Bayes theorem. If the physical quantities of interest (e.g. geometric mean and variance of a lognormal distribution), are represented by a vector f, and the measurement process furnishes numbers represented by a vector y, then the Bayesian expression for the updated probability distribution of f is $P_{post}(f|y) = \frac{P_o(f)P_L(y|f)}{P(y)}$, where $P_o(f)$ is the probability distribution of f prior to making any measurements, $P_L(y|f)$ is the likelihood that given the true value f the measurement y is observed, $P(y)$ is the probability that the measurement y is observed, and $P_{post}(f|y)$ is the updated probability that the physical quantity of interest is y, given that measurements y are observed. In Kandlikar and Ramachandran (1999) the Bayes formulation is combined with Monte Carlo simulations to provide the updated probability distribution of the physical quantities being determined given assumptions on probability distributions of f prior to measurement, and the observations on the model output y with their corresponding expected experimental errors. The updated probability density $P_{post}(f|y)$ is used to determine the best estimates of f.

Voutilainen *et al*. (2000) introduced a statistical inversion method of aerosol size measurement data, in which both the observations and the unknown parameters are treated as random variables. They construct a realistic posterior model for the aerosol size distribution function by using the Baye's Theorem, assuming that the measurements obey Poisson statistics and that the solution is a smooth nonnegative function.

2.4.3 Inversion of Tandem DMA Measurements

The measurement signal of a TDMA, i.e. the measurement distribution function (MDF), is the particle concentration at the TDMA outlet related to a size-changing function set at the instrument. As the MDF is only a skewed and smoothed integral transform of the particle's actual growth factor probability density function (GF-PDF) an inversion algorithm has to be applied to the MDF of TDMA measurements to retrieve the GF-PDF.

TDMA data analysis approaches seek to determine the mean size-change of the sample, to provide the number fractions of particles in different GF ranges and to retrieve the correct shape of the GF-PDF in detail. The simplest method is to use the MDF without any data inversion to determine integral properties of the GF-PDF (e.g. Liu *et al*., 1978; Weingartner *et al*., 2002), but, this approach does not fulfil any specification expect for samples exhibiting monomodal growth with limited spread between individual particles, where the MDF can be used to determine the mean GF. A second approach is to invert for the smearing and skewing effect of the second DMA only, in order to recover the particle size distribution after treatment (e.g. Cocker *et al*., 2001; Stratmann *et al*., 1997; Voutilainen *et al*., 2000). This approach fulfils all specifications because the particle size distribution after treatment resembles the GF-PDF except for some smoothing caused by the finite width of the size corresponding to particles selected with the first DMA. The third class of methods aims to recover the actual GF-PDF by inversion of the MDF using a complete TDMA forward function (e.g. Cubison *et al*., 2005; Stolzenburg & McMurry, 1988). This class of methods satisfies all criteria as closely as possible within the limits imposed by the measurement uncertainties and inversion algorithm itself.

The TDMAfit algorithm (Stolzenburg & McMurry, 1988) is the most widespread inversion approach. It describes the GF-PDF as a superposition of multiple Gaussian distributions, whereas the mean GF, standard deviation and number fraction in each Gaussian mode are varied until the observed MDF is reproduced by sending the resulting GF-PDF through the forward function of the TDMA. However, convergence of fitting multiple modes is not robust in cases with largely overlapping modes or shoulders, and successful convergence may depend on the initial guess. This makes automated data analysis of large data sets difficult.

The optimal estimation method (OEM), introduced by Cubison et al. (2005), uses a quasi-inverse matrix of the TDMA kernel function in order to retrieve the values of the GF-PDF at discrete bin positions. This method is very efficient, returning unambiguous

results for given retrieval bins and provides tools for a thorough uncertainty analysis. However, constraints such as keeping the GF-PDF positive cannot be applied because it is a linear method. This can lead to oscillations with alternating positive and negative values in the retrieved GF-PDF, which propagate outside of the support of the MDF, if the chosen resolution is too high. Gysel *et al*. (2009) develop an alternative TDMA data inversion approach, which is a robust and automated data inversion algorithm, which has successfully been tested and applied to large HTDMA data sets in recent laboratory and field studies (Allan et al., 2008; Gysel et al., 2007; Meyer et al., 2008; Sjogren et al., 2008).

Table 2. 1 Inversion Techniques

Inversion Technique	References	Constraints /a priori Information	Comments
I. Linear methods			
1. Least-squares		None	Very unstable in presence of measurement error
2. Constrained least-squares	Philips (1962),	Second difference,	Solution could take on negative values
		first difference or deviation from trial solution	
	Twomey (1963),		
	Twomey (1977),	is minimised	
	Rizzi et al. (1982)		
3. Tikhonov regularisation	Tikhonov and Arsenin (1977),		
	Hansen (1992)		
	Hansen and O'Leary (1993)		
a.	Crump and Seinfeld (1982)	Norm of second derivative minimized	
b.	Yee (1989)	Shannon - Jaynes entropy maximised	Intrinsically positive solution
c.	Lesnic et al (1995)	Norm of first derivative minimised; positivity of solution	
d. Selection of λ	Wahba (1977),	Minimise the generalized cross validation (GCV) function	GCV function can have a flat minimum and can be difficult to locate
	Golub et al. (1979),		
	Crump and Seinfeld (1982)		
e.	Ramachandran et al. (1996)	Discrepancy principle	Computationally simple, but can oversmooth solution
f.	Hansen (1992),	L-curve method	Reliable but computationally intensive
	Hansen and O'Leary (1993),		
	Lloyd et al. (1997a)		

Table 2. 1 Continued

Inversion Technique	References	Constraints /a priori Information	Comments
4. Synthesis of basis functions			
a. Eigenvalue decomposition	Twomey (1963), Twomey (1975), Capps et al. (1982)	Disregard of replace problematic eigen values using filters	Measurements chosen to remove singularity
b.	Curry (1989)	Smoothness constraint	
c. Second derivative expressed as sum of orthogonal functions	Ramachandran and Leith (1992)	Norm of second derivative minimised	Intrinsically positive solution
4. Synthesis of basis functions a. Eigenvalue decomposition	Twomey (1963),	Disregard of replace	Measurements chosen to remove singularity
	Twomey (1975),	problematic eigen values using filters	
	Capps et al. (1982)		
b.	Curry (1989)	Smoothness constraint	
c. Second derivative expressed as sum of orthogonal functions	Ramachandran and Leith (1992)	Norm of second derivative minimised	Intrinsically positive solution
d. Singular value decomposition	Bertero et al. (1985, 1986),	Disregard or replace problematic singular values using filters	Allows choice of measurements to avoid singularity; smoothing
	Arridge et al. (1989),		
	Viera and Box (1985, 1987)		

Table 2. 1 Continued

Inversion Technique	References	Constraints /a priori Information	Comments
II. Non-linear methods			
1. Chahine method	Chahine (1968), Grassl (1971), Santer and Herman (1983), Ferri et al. (1989)	Initial guess solution is positive	Final solution always positive. High - frequency oscillations or choppiness in solution
2. a. Twomey's method	Twomey (1975), Hitzzenberger and Rizzi (1986),	Initial guess solution is positive	
b.	Markowski (1987), Roth and Filippov (1997)	Initial guess solution is positive. Smoothness constraint	
c.	Winklmayr et al. (1990)	Use smoothed kernel fuctions	
III. Extreme value estimation	Paatero (1991)		

Chapter 3. Methodology

Chapter 3. Methodology

3.1 Methodology

Aerosol size distribution measurements require having the appropriate instrumentation (hardware) and also the theoretical framework (models) of the individual system components, as shown in Figure 3.1. As already, mentioned in § 2.???, the basic components of an electrical mobility spectrometer are the charger, the classifier and the counter. Part of this study focuses on the modeling of the transfer function of a Multiple Monodisperse Outlet DMA, including the derivation of a theoretical framework towards predicting the response of an aerosol size measurement system consisting of a Dual-MO DMA. After these models are finalized, an inversion algorithm will be developed for retrieving size distribution data from SMPS and TDMA measurements. Herein, we present the derivation of the MMO-DMA transfer function and the Knutson inversion method, which will be the basis for the development of a novel inversion code for the MMO-DMA.
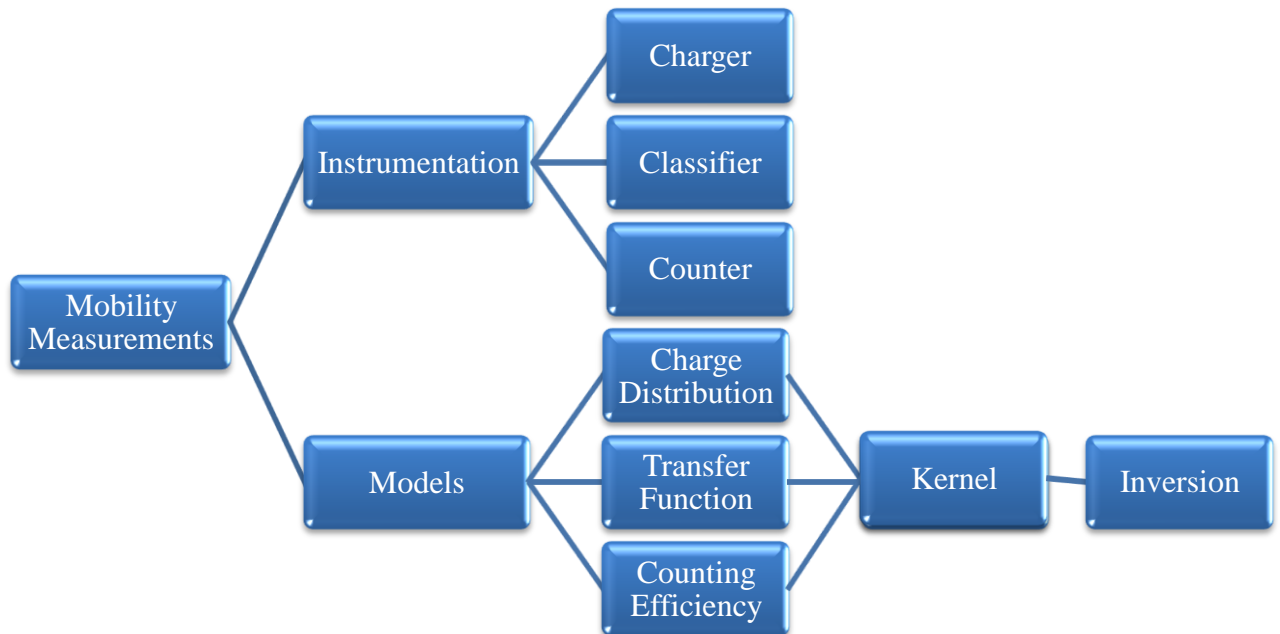

Figure 3. 1 Schematic diagram of the Methodology

3.2 Current Achievements and Future Work Plan

The transfer function of the MMO-DMA for non-diffusing particles, Ω_{nd_i}, can be written in dimensionless form as:

$$\Omega_{nd_i} = \frac{1}{2\beta_i(1-\delta_i)} \quad \begin{aligned} &\left\{\left|\tilde{Z}_{p_i} - (1+\beta_i)\right| - \left|\tilde{Z}_{p_i} - (1+\beta_i\delta_i)\right| \\ &-\left|\tilde{Z}_{p_i} - (1-\beta_i\delta_i)\right| + \left|\tilde{Z}_{p_i} - (1-\beta_i)\right|\right\} \end{aligned} \tag{9}$$

where $\beta_i = \frac{Q_a+Q_{s_i}}{Q_{sh_i}+Q_{m_i}}$ and $\delta_i = \frac{Q_{s_i}-Q_a}{Q_{s_i}+Q_a}$ are the dimensionless flow parameters that correspond to the *ith* exit ($Q_a, Q_{s_i}, Q_{sh_i}, Q_{m_i}$ the aerosol, sample, sheath and excess flow rate at the *ith* exit), and $\tilde{Z}_{p_i} \equiv \frac{Z_p}{Z_{p_i}^*}$ the dimensionless variable defined as the ratio of the particle electrical mobility to the midpoint electrical mobility for each monodisperse-particle outlet (Giamarelou and Biskos, 2011).

The equation above is similar to that derived by Stolzenburg (1988) for the single monodisperse-particle outlet DMA, with the difference that all the non-dimensional variables correspond to the *ith* exit as described at the above relations. Using the derived transfer function one can optimize the design (i.e. the number and the location of the exits) of any MMO-DMA, and invert the data of mobility spectrometers that employ such DMAs.

When the particle diffusion is taken into account the transfer function of the *ith* exit of the MMO-DMA for diffusing particles is given by (Giamarelou and Biskos, 2011)

$$\Omega_{d_i} = \frac{\sigma_i}{\sqrt{2}\beta_i(1-\delta_i)} \left\{ -\mathcal{E}\left(\frac{\tilde{Z}_{p_i}-(1-\beta_i\delta_i)}{\sqrt{2}\sigma_i}\right) + \mathcal{E}\left(\frac{\tilde{Z}_{p_i}-(1-\beta_i)}{\sqrt{2}\sigma_i}\right) \\ +\mathcal{E}\left(\frac{\tilde{Z}_{p_i}-(1+\beta_i)}{\sqrt{2}\sigma_i}\right) - \mathcal{E}\left(\frac{\tilde{Z}_{p_i}-(1+\beta_i\delta_i)}{\sqrt{2}\sigma_i}\right) \right\} \tag{10}$$

where σ_i is the standard deviation of the transfer function. Here $\mathcal{E}$ is the integral of the error function defined as $\mathcal{E}(x) \equiv \int_0^x \mathrm{erf}(u)\, du = x\, \mathrm{erf}(x) + \frac{1}{\sqrt{\pi}}\exp(-x^2)$, where the standard error function is given by $\mathrm{erf}(x) \equiv \frac{2}{\sqrt{\pi}}\int_0^x \exp(-u^2)du$.

Once, the transfer function of the MMO-DMA is ready, and the response of the spectrometer or the TDMA system employing such DMAs is modeled, the algorithm for inverting the data from mobility spectrometers and TDMA systems when such DMAs are

employed. A first approach for the derivation of the inversion code will be the one basd on the Knutson (1976_ inversion method, described below.

The DMA is usually operated at high resolution, so that nonzero values of transfer function, Ω, occur only in a very narrow range of electrical mobility, Z_p, centered around centroid electrical mobility, Z_p^*. Knutson (1976) therefore assumes that $N(x)$ and $\phi_v(x)$ are approximate constant over the corresponding range of electrical mobilities, thus the response of the sensor is given by:

$R(V) \equiv q_a \sum_{v=1}^{\infty} W_v \phi_v(x^*) N(x^*) \int_0^{\infty} \Omega \, dx$, where x^* are the values of x corresponding to Z_p^*. The size of those particles leaving the DMA with the same number of charges, i.e., v, is nearly equal to x^*. Therefore, the sensor response can be written on the equivalent form

$R(V) \equiv \frac{2q_a q_s}{q_c + q_m} \sum_{v=1}^{\infty} W_v \phi_v(x^*) N(x^*) \widehat{K}(x^*) f(x^*)$, where $f(x) = \left(\frac{d\widehat{K}}{dx}\right)^{-1}$ and $\widehat{K}$ is the mobility of singly charged particles of size x. Knutson (1976) reports that for particles larger than 0.5 μm four terms are sufficient:

$R(V) \equiv \frac{2q_a q_s}{q_c + q_m} \sum_{v=1}^{4} W_v \phi_v(x_{i,v}^*) N(x_{i,v}^*) \widehat{K}(x_{i,v}^*) f(x_{i,v}^*)$, where i denotes the *ith* voltage step.

Chapter 4. Summary and Timeline

Chapter 4. Summary and Timeline

Measurements of mobility size in tandem with other properties enable a far more detailed characterization of aerosol physical and chemical properties than can be achieved with one measurement only. Such measurements can establish relationships between different measurements of size, can offer information on particle properties such as shape, density, hygroscopicity, volatility and reactivity.

The aerosol measurement signals obtained from a electrical mobility spectrometers or TDMA systems required inversion algorithms in order to retrieve the size distribution function of the sample aerosol and the measured intrinsic properties, respectively. Prior, the response of the system has to be modeled taking into acount the charge distribution, the transfer function of the classifier (or classiers in the case of TDMA systems), and the counter efficiency.

As shown in Figure 4.1, this research has started in November 2009, with the study of the DMA (and the TDMA) transfer function and resolution, which was the base for the development of the MMO-DMA transfer function (first paper, submitted on March 2011, at Aerosol Science and Technology). The next target is the optimization of a MMO-DMA design with two monodisperse outles (second paper, to be submitted by July 2011). In parallel, the instrument response of an SMPS and a TDMA that will include this newly developed MMO-DMA are studied with the objective of developing the inversion algorithms for interpreting the measurements from these systems. The modeling of the SMPS and the TDMA response is the intermediate step for the development of the inversion code (third paper January 2012), that will enable analysis of the hygroscopicity and volatility TDMA measurements that are already underway (November 2012; fourth paper).
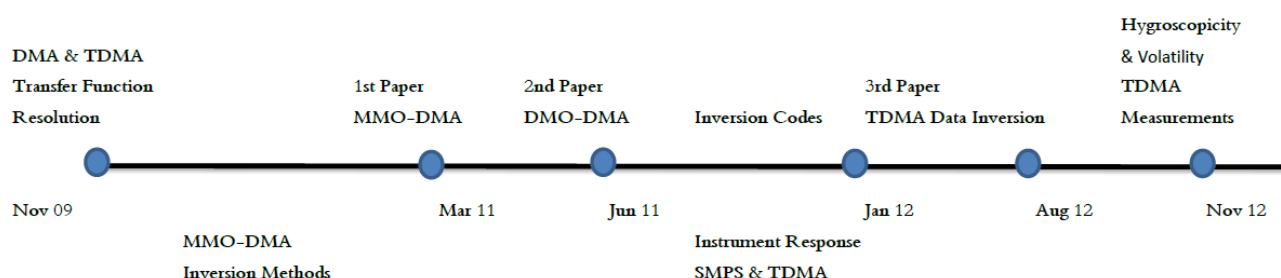

Figure 4. 1 Research Timeline

Bibliography

Bibliography

Alofs, D.J., Balakumar, P., 1982, Inversion to Obtain Aerosol Size Distributions from Measurements with a Differential Mobility Analyzer, *J. Aerosol Sci. 13:*513-527.

Alonso, M., 2002, Reducing the diffusional Spreading rate of a Brownian particle by an appropriate non-uniform external force field, *J. Aerosol Sci. 33*:439-450.

Allan, J. D., Baumgardner, D., Raga, G. B., Mayol-Bracero, O. L., Morales-García, F., García-García, F. *et al.* , 2008, Clouds and aerosols in Puerto Rico—a new evaluation. *Atmospheric Chemistry and Physics*, *8*: 1293–1309.

Allen, M.D., Raabe, O.G., 1985, Slip Correction Measurements of Spherical Solid Aerosol Particles in an Improved Millikan Apparatus, *Aerosol Sci. and Technol. 4*: 269-286.

Baron, A. and Willeke, K., 2001, "Aerosol Fundamentals", in *Aerosol Measurements: Principles, Techniques, and Applications*, Second Edition, Baron, A. and Willeke, K. (Eds.), Wiley-InterScience, New York.

Bilde, M., Pandis, S. N., 2001, Evaporation rates and vapor pressures of individual aerosol species formed in the atmospheric oxidation of α- and β-pinene. *Environmental Science and Technology*, *35*, 3344–3349.

Biskos, G., Reavell, K., Collings, N., 2005, Description and Theoretical aNalysis of a Differential Mobility Spectrometer, *Aerosol Sci. and Technol.39:*527-541.

Brown, W.K. and Wohletz, K.H., 1995, Derivation of the Weibull distribution based on physical principles and its connection to the Rosin-Rammler and lognormal distribution. *J. Appl. Phys. 78*: 2758-2763.

Brunelli, N. A., Flagan, R. C., Giapis, K. P., 2009, Radial differential mobility 580 analyzer for one nanometer particle classification, *Aerosol Sci. Technol.,* 43:53–39.

Buscher, P., A. Schmidt-Ott, and A. Wiedensohler. 1994. Performance of a unipolar square-wave diffusion charger with variable Nt product. J. *Aerosol Sci.* 25:651-663.

Chahine, M. T. (1968) Determination of the temperature profile in an atmosphere from its outgoing radiance. *J. Opt. Soc. Am.* 58, 1634-1637.

Chen, D.R. and Pui, D.Y.H., 1995, Numerical Modeling of the Performance of the Differential Mobility Analyzer for Nanometer Aerosol Measurements, *J. Aerosol Sci.,26:* S141-S142.

Chen, D.R. and Pui, D.Y.H., 1997, Numerical Modeling of the Performance of Differential Mobility Analyzers for Nanometer Aerosol Measurements, *J. Aerosol Sci., 28:*985-1004.

Chen, D.R., Pui, D.Y.H, Hummes, D., Fissan, H., Quant, F.R., Sem, G.J., 1998, Design and Evaluation of a Nanometer Aerosol Differential Mobility Analyzer (Nano-DMA), *J. Aerosol Sci.29*: 497-509.

Chen, D.R., Pui, D.Y.H, Mulholland, G., Fernandez, M., 1999, Design and Testing of an Aerosol/Sheath Inlet for High Resolution Measurements with TSI-DMA, *J. Aerosol Sci. 30:* 983-999.

Chen, D.R., Li, W., Cheng, M.D., 2007, Development of a Multiple-Stage Differential Mobility Analyzer (MDMA), *Aerosol Sci. & Technol.* 41:217-230.

Clement, C. F. & Harrison, R. G., 1991, Charge distributions on aerosols. *Proceedings of the 8th International Conference of Electrostatics 118*, 275-280.

Cocker, D. R., III, Whitlock, N. E., Flagan, R. C., Seinfeld, J. H., 2001, Hygroscopic properties of Pasadena, California aerosol. *Aerosol Sci. & Technol. 35*: 637–647.

Collins, D.R., Nenes, A., Flagan, R.C., Seinfeld, J.H., 2000, The Scanning Flow, DMA, *J. Aerosol Sci., 31:*1129-1144.

Cooper, D. W. and Spielman, L. A. (1976) Data inversion using nonlinear programming with physical constraints: aerosol size distribution measurement by impactors. *Atmos. Envir*. 10, 723-729.

Covert, D. S., Heintzenberg, J., and Hansson, H. C. , 1990, Electro–Optical Detection of External Mixtures in Aerosols, *Aerosol Sci. Technol. 12*:446– 456.

Crump, J.G., Seinfeld, J.H., 1982, A new Algorithm for Inversion of Aerosol Size Distribution Data, *Aerosol Sci. & Technol. 1:*15-34.

Cubison, M., Coe, H.., Gysel, M., 2005, Retrieval of hygroscopic tandem DMA measurements using an optimal estimation method. *J. Aerosol Sci., 36*: 846–865.

Dassios, K. G., Pandis, S. N., 1999, The mass accommodation coefficient of ammonium nitrate aerosol. *Atmospheric Environment*, *33*, 2993–3003.

DeCarlo, P. F., Slowik, J. G., Worsnop, D. R., Davidovits, P., Jimenez, J. L., 2005, Particle Morphology and Density Characterization by Combined Mobility and Aerodynamic Diameter Measurements. Part 1: Theory, *Aerosol Sci. Technol. 38*:1185–1205.

de Juan, L., de la Mora, J.F., 1998, High Resolution Size Analysis of Nanoparticles and Ions: Running a Vienna DMA of Near Optimal Length at Reynolds Numbers up to 5000, *J. Aerosol Sci., 29:*617-626.

de la Mora, J.F., de Juan, L., Eichler, T., Rossel, J., 1998, Differential mobility analysis of molecular ions and nanometer particles, *Trends in analytical chemistry, 17*: 328-339.

de la Mora, J.F., 2002, Diffusion broadening in converging differential mobility analyzers, *J. Aerosol Sci.,33:*411-437.

Dick, W. D., McMurry, P. H., 2007, Mulitangle Light-Scattering Measurements of Refractive Index of Submicron Atmospheric Particles, *Aerosol Sci. Technol. 41*:549–569.

Dockery, D.W., Pope, C. A. ,1994, Acute Respiratory Effects of Particulate Air Pollution, *Ann. Rev. Public Health, 15*:107–132.

Eichler, t., de Juan, L., de la Mora, F.J., 1998, Improvements of the Resolution of TSI's 3071 DMA via Redesigned Sheath Air and Aerosols Inlets, *Aerosol Sci. & Technol., 29:* 39-49.

Endo, Y., Fukushima, N., Tashiro, S., Kousaka, Y., 1997, Performance of a Scanning Differential Mobility Analyzer, *Aerosol Sci. & Techn.*, 26:43-50.

Enting, I. G. and Newsam, G. N. (1990) Atmospheric constituent inverse problems: Implications for baseline monitoring. *J. Atmos. Chem*. 11, 69-87.

Ferri, F., Giglio, M. and Perini, U. (1989) Inversion of light scattering data from fractals by the Chahine iterative algorithm. *Appl. Opt*. 28, 3074-3082.

Fissan, H. J., Helspcr, C., Thielen, H. J.,1982, Determination of particle size distributions by means of an electrostatic classifier. *J. Aerosol Sci.* 14, 354.

Fissan, H., Hummes, D., Stratmann, F., Buscher, P., Neumann, S., Pui, D.Y.H., Chen, D., 1996. Experimental Comparison of Four Differential Mobility Analyzers for nanometer Aerosol Measurements, *Aerosol Sci. & Technol., 24,* 1 – 13.

Flagan, R.C., 1998, History of Electrical Aerosol Measurements, *Aerosol Sci. &* 594 *Techn*., 28:301-380

Flagan, R., 2001, "Electrical Techniques", in *Aerosol Measurements: Principles, Techniques, and Applications*, Second Edition, Baron, A. and Willeke, K. (Eds.), Wiley-InterScience, New York.

Fuchs, N. A. & Lissowski, P., 1956, The charging of aerosols by ionic diffusion. *Journal of Colloid & Interface Science*, *11*, 107-108.

Geller, M., Biswas, S., Sioutas, C., 2006, Determination of Particle Effective Density in Urban Environments With a Differential Mobility Analyzer and Aerosol Particle Mass Analyzer, *Aerosol Sci. Technol.* 40:709–723.

Gentry, J. W. (1972) *J. Aerosol Sci.* 3, 65.

Giamarelou, M., Biskos,G., 2011, The Multiple Monodisperse Outlet Differential Mobility Analyzer: Derivation of its Transfer Function and Resolution, *Aerosol Sci. & Technol.,* submitted.

Golub, G. H., Heath, M. and Wahba, G. (1979) Generalized cross-validation as a method for choosing a good ridge parameter. T*echnometrics* 21, 215-223.

Gonda, I. (1984) On inversion of aerosol size distribution data. Letter to the editor. *Aerosol Sci.* T*echnol.* 3, 345-346.

Grassl, H. (1971) Determination of aerosol size distributions from spectral attenuation measurements. *Appl. Opt.* 10, 2534-2538.

Gunn, R., 1955, The statistical electrification of aerosols by ionic diffusion. *J. Colloid & Interface Science*, *10*, 107-119.

Gysel, M., Weingartner, E., Baltensperger, U., 2002, Hygroscopicity of aerosol particles at low temperatures. 2. Theoretical and experimental hygroscopic properties of laboratory generated aerosols. *Environmental Science and Technology*, *36:* 63–68.

Gysel, M., Crosier, J., Topping, D., Whitehead, J., Bower, K., Cubison, M. et al., 2007, Closure study between chemical composition and hygroscopic growth of aerosol particles during TORCH2. *Atmospheric Chemistry and Physics*, *7*: 6131–6144.

Gysel, M., McFiggans, G.B., Coeb, H., 2009, Inversion of tandem differential mobility analyser (TDMA) measurements, *J. Aerosol Sci., 40*: 134-151.

Haaf, W., 1980, Accurate Measurements of Aerosol Size Distribution - II. Construction of a New Plate Condenser Electric Mobility Analyzer and First Results, *J. Aerosol Sci, 11*: 201-212.

Hagwood, C., Sivathanu, Y., Mulholland, G., 1999, The DMA Transfer Function with 601 Brownian Motion a Trajectory/Monte-Carlo Approach, *J. Aerosol Sci. & Techn*., 602 30:40-61.

Hansen, P. C. (1992) Analysis of discrete ill-posed problems by means of the L-curve. *SIAM Rev*. 34, 561-580.

Hansen, P. C. and O'Leary, D. O. (1993) The use of the L-curve in the regularisation of discrete ill-posed problems. *SIAM J. Sci. Comput*. 14, 1487-1503.

Hinds, W. C. (1999). *Aerosol Technology: Properties, Behavior, and Measurement of Airborne Particles* (2 ed.). John Wiley & Sons.

Hitzenberger, R. and Rizzi, R. (1986) Retrieved and measured aerosol mass size distributions: a comparison. *Appl. Opt*. 25, 546-553

Heintzenberg, J., Okada, K., Lui, B. P., 2002, Distribution of Optical Properties Among Atmospheric Submicrometer Particles of Given Electrical Mobilities, *J. Geophys. Res. Atmospheres* 107:4107–4115.

Heintzenberg, J., Okada, K., Trautmann, T., and Hoffmann, P., 2004, Modeling of the Signals of an Optical Particle Counter for Real Nonspherical Particles, *Appl. Opt.* 43:5893–5900.

Hering, S., McMurry, P. H., 1991, Optical Counter Response to Monodisperse Atmospheric Aerosols, *Atmos. Environ., 25A*:463–468.

Hewitt, G. W. 1957. The charging of small particles for electrostatic precipitation. *Trans. Am. Inst. Elect. Engr.* 76:300-306.

Hoppel, W.A., 1978, Determination of the Aerosol Size Distribution from the Mobility Distribution of the Charged Fraction of Aerosols, *J. Aerosol Sci. 9:*41-54.

IPCC, 2007, *Climate Change 2007: IPCC Fourth Assessment Report (AR4)*. Cambridge University Press.

Johnson, G. R., Ristovski, Z., Morawska, L., 2004, Method for measuring the hygroscopic behaviour of lower volatility fractions in an internally mixed aerosol, *J. Aerosol Sci.*, *35*, 443–455.

Joutsensaari, J., Vaattovaara, P., Vesterinen, M., Hämeri, K., Laaksonen, A., 2001, A novel tandem differential mobility analyzer with organic vapor treatment of aerosol particles. *Atmospheric Chemistry and Physics*, *1*(1), 51–60.

Kandlikar, M., Ramachandran, G., 1999, Inverse Methods for Analysing Aerosol Spectrometer Measurements: A Critical Review, *J. Aerosol Sci. 30:*413-437.

Knutson, E. O., Whitby, K. T., 1975, Aerosol Classification by Electric Mobility: 608 Apparatus, Theory, and Applications, *J.Aerosol Sci.* 6: 443-451.

Knutson, E. O., 1976, Extended Electric Mobility Method for Measuring Aerosol Particle Size and Concentration, In *Fine Particles* (Edited by Liu, B. Y. H.) p. 739-762. Academic Press, New York.

Kousaka, Y., Okuyama, K., Adachi, M., 1985, Determination of Particle Distribution of Ultra-Fine Aerosols Using Differential Mobility Analyzer, J., *Aerosol Sci. & Techol.*, 4:209-225.

Kousaka, Y., Okuyama, K., Adachi, M., Mimura, T., 1986, Effect of Brownian Diffusion on Electrical Classification of Ultrafine Aerosol Particles in Differential Mobility Analyzer, *J. Chem. Eng. Japan*, 19: 401-407.

Kulkarni, P. and Wang, J., 2006, New fast integrated mobility spectrometer for real-time measurement of aerosol size distribution—I: Concept and theory, *J.Aerosol Sci.*, 37: 1303-1325.

Lesnic, D., Elliot, L. and Ingham, D. B. (1995) An inversion method for the determination of the particle size distribution from diffusion battery measurements. *J. Aerosol Sci.* 26, 797-812.

Liu, B. Y. H, Pui, D. Y. H., 1974, A Submicron Aerosol Standard and the Primary, Absolute Calibration of the Condensation Nuclei Counter, *J. Colloid Interface Sci.* 47, 155-171.

Liu, B. Y. H., Pui, D. Y. H., 1974a, Electrical neutralization of aerosols. *J.Aerosol Sci.*, *5*, 465-472.

Liu, B. Y. H. & Pui, D. Y. H. ,1974b, Equilibrium bipolar charge distribution of aerosols. *Journal of Colloid & Interface Science*, *49*, 305-312.

Liu, B. Y. H., Pui, D. Y. H., Whitby, K. T., Kittelson D. B., Kousaka, Y., McKenzie, R. L., 1978, The aerosol mobility chromatograph: a new detector for sulfuric acid aerosols. *Atmos. Envir.* 12, 99-104.

Lissowski, P. (1940) *Acta. phys. chim. URSS* 13, 157.

Lloyd, J. J., Taylor, C. J., Lawson, R. S. and Shields, R. A. (1997a) The use of the L-curve method in the inversion of diffusion battery data. *J. Aerosol Sci.* 28, 1251-1264.

Loscertales, I., 1998, Drift Differential Mobility Analyzer, *J.Aerosol Sci.*,*29*: 1117-1139.

Martinez-Lozano, P., de la Mora, J.F., 2006a, Resolution improvements of a nano-DMA operating transonically, *J.Aerosol Sci.*, *37*: 500-512.

Martinez-Lozano, P., Labowsky, M., de la Mora, J.F., 2006b, Experimental tests of a nano-DMA with no voltage change between aerosol inlet and outlet slits, *J.Aerosol Sci.*, *37*: 1629-1642.

McMurry, P. H., Takano, H., Anderson, G. R., 1983, Study of the ammonia (gas)-sulfuric acid (aerosol) reaction rate. *Envir. Sci. Technol.* 17, 347.

McMurry, P.H., 2000, A review of atmospheric aerosol measurements, *Atmos.* 619 *Environ.,* 34:1959-1999.

McMurry, P. H., Wang, X., Park, K., Ehara, K., 2002, The Relationship between Mass and Mobility for Atmospheric Particles: A New Technique for Measuring Particle Density, *Aerosol Sci. Technol. 36*:227–238.

Meyer, N. K., Duplissy, J., Gysel, M., Metzger, A., Weingartner, E., Alfarra, M. R. et al.,2008, Analysis of the hygroscopic and volatile properties of ammonium sulphate seeded

and un-seeded SOA particles. *Atmospheric Chemistry and Physics Discussions*, *8:* 8629–8659.

Mohnen, V. A., 1977, Formation, nature, and mobility of ions of atmospheric importance. *Proceedings of the 5th International Conference on Atmospheric Electricity*, 1.17.

Naoe, H., Okada, K., 2001, Mixing Properties of Submicrometer Aerosol Particles in the Urban Atmosphere—With Regard to Soot Particles, *Atmos. Environ. 35*: 5765–5772.

NRC, 1993, *Protecting Visibility in National Parks and Wilderness Areas*. National Academy Press, Washington, D.C.

Oberdörster, G., 2000, Toxicology of Ultrafine Particles: *In Vivo* Studies, *Philosophical Transactions of the Royal Society of London,* 358: 22719–22740.

Okada, K., Heintzenberg, J., 2003, Size Distribution, State of Mixture and Morphology of Urban Aerosol Particles at Given Electrical Mobilities, *J. Aerosol Sci. 34*:1539–1553.

Paatero, P., 1991, Extreme value estimation, a method for regularizing ill-posed inversion problems. In *Ill-posed Problems in Natural Sciences*. Proc. of Int. Conf., Moscow VSP Utrecht, The Netherlands.

Paulsen, D., Weingartner, E., Alfarra, M. R., Baltensperger, U., 2006, Volatility measurements of photochemically and nebulizer-generated organic aerosol particles. *J. Aerosol Sci.*, *37*, 1025–1051.

Peters, A., Wichmann, H. E., Tuch, T., Heingrich, J., and Heyder, J., 1997, Respiratory Effects are Associated with the Number of Ultrafine Particles, *Am. J. Respir. Crit. Care Med., 155*:1376–1383.

Philippin, S., Wiedensohler, A., Stratmann, F., 2004, Measurements of non-volatile fractions of pollution aerosols with an eight-tube volatility tandem differential mobility analyzer (VTDMA-8). *J. Aerosol Sci., 35*, 185–203.

Phillips, D. L., 1962, A technique for the numerical solution of certain integral equations of the Þrst kind. *J. Ass. Comp. Mach.* 9, 84-97.

Pollak, L. W. and Metnieks, A. L. (1962) *Geofis pura appl.* 53, 111.

Pourpix, M., Daval, J., 1990. Electrostatic Precipitation of Aerosol on Wafers, a New 621 Mobility Spectrometer. In S. Masuda and K. Takahashi (eds.), *Aerosols: Science,* 622

Industry, Health and Environment (Proceedings of the Third Int. Aerosol Conference, 24-27 Sept, 1990, Kyoto, Japan), Vol. II, Pergamon Press, Oxford, UK.

Pourprix, M., 1994. Sélecteur de particules chargées, a haute sensibilité, Brevet francais No. 94 06273, 24 Mal.

Plomp, A., ten Brink, H. M., Spoelstra, H., van de Vate, J. F., 1982, A high resolution electrical mobility aerosol spectrometer (MAS). *J. Aerosol Sci.* 14, 363.

Prupacher, H.R. and Klett, J.D., 1980, *Microphysics of Clouds and Precipitation*, Boston: Reidel.

Pui, D.Y.H., 1996, Direct-reading instrumentation for workplace aerosol measurements – A review. *Analyst 121*:1215-1224.

Rader, D.J., McMurry, P.H., 1986, Application of the Tandem Differential Mobility Analyzer to Studies of Droplet Growth or Evaporation, *J. Aerosol Sci.17*: 771-787.

Rader, D. J., McMurry, P. H. Smith, S., 1986b, Evaporation rates of monodisperse organic aerosols in the 0.02 to 0.2/am diameter range. *Aerosol Sci. Technol.,* 6:247–260.

Ramachandran, G., Kandlikar, M., 1996, Bayesian analysis for inversion of aerosol size distribution data. *J. Aerosol Sci*. 27, 1099-1112.

Ramiro, E., Ramiro, F., Sanchez, M., Lazcano, J.A., de Juan, J., de la Mora, J.F., 2003, A DMA of Inverted Geometry for High Reynolds Number Operation, *Abstracts of European Aerosol Conference,* S915-S916.

Ramm, A.G., 2005, *Inverse problems: Mathematical and Analytical Techniques with Applications to Engineering*, Springer, New York.

Randall, D. A., Wood, R. A., Bony, S., Colman, R., Fichefet, T., Fyfe, J., Kattsov, V., Pitman, A., Shukla, J., Srinivasan, J., Stouffer, R. J., Sumi, A., Taylor, K. E., 2007, Climate Models and Their Evaluation, in *Climate Change 2007: The Physical Science Basis, Contribution of Working Group I to the Fourth Assessment Report of the Intergovernmental Panel on Climate Change*, Cambridge University Press, Cambridge, UK and New York, NY, USA, 590–662.

Rizzi, R., Guzzi, R. and Legnani, R. (1982) Aerosol size spectra from spectral extinction data: the use of a linear inversion method. *Appl. Opt*. 21, 1578-1587.

Rosin, P. and Rammler, E., 1933, The laws governing the fineness of powdered coal. *J. Inst. Fuel 7*: 29-36.

Rosell- Llompart, J., Loscertales, I. G., Bingham, D., de la Mora, J.F., 1996, Sizing Nanoparticles and Ions with a Short Differential Mobility Analyzer, *J. Aerosol Sci.* 27:695-719.

Roth, P. and Filippov, A. V. (1996) *In-Situ* ultraÞne particle sizing by a combination of pulsed laser heatup and particle thermal emission. *J. Aerosol Sci.* 27, 95-104.

Salm, J. (1983). The Effect of Turbulent and Molecular Diffusion in the Spectrometer of Air Ions, *Proc. In Atmospheric Electricity*, edited by L. H. Ruhnke and J. Latham. A. Deepak Publishing, Hampton, pp. 61-64.

Salm, J., 2000, Diffusion Distortions in a Differential Mobility Analyzer: The shape of Apparent Mobility Spectrum, *Aerosol Sci. & Technol, 32*:602-612.

Santer, R. and Herman, M. (1983) Particle size distributions from forward scattered light using Chahine inversion scheme. *Appl. Opt*. 22, 2294-2302.

Santos, J.P., Hantanon, E., Ramiro, E., Alonso, M., 2009, Performance evaluation of a high-resolution parallel-plate differential mobility analyzer, *Atmos. Chem. Phys., 9*:2419-2429.

Seol, K. S., Yabumoto, J., Takeuchi, K., 2002, A Differential Mobility Analyzer with Adjustable Column Length for Wide Particle-Size-Range Measurements, *J. Aerosol Sci.,* 33:1481–1492.

Schmidt-Ott, A., P. Schurtenberger, and H. C. Siegmann. 1980. Enormous yield of photoelectrons from small particles. *Phys. Rev. Lett.* 45:1284-1287.

Shannon, C. E. and Weaver, W. (1962) *The Mathematical theory of Communication*. University of Illinois Press, Urbana, IL.

Sjogren, S., Gysel, M., Weingartner, E., Alfarra, M.R., Duplissy, J., Cozic, J., et al., 2008, Hygroscopicity of the submicrometer aerosol at the high-alpine site Jungfraujoch, 3580m a.s.l., Switzerland. *Atmospheric Chemistry and Physics*, 8: 5715–5729.

Song, D.K., Dhaniyala, S., 2007, Change in distributions of particle positions by Brownian diffusion in a non-uniform external field, *J. Aerosol Sci. 38:*444-454.

Stolzenburg, M., 1988, PhD Thesis, University of Minnesota, St. Paul, MN.

Stolzenburg, M., McMurry, P.H.,1988, *TDMAfit user's manual*. Technical Report, PTL Publication No. 653, University of Minnesota, Department of Mechanical Engineering, Particle Technology Laboratory.

Stratmann, F. , Kauffeldt, Th. , Hummes, D. and Fissan, H., 1997, 'Differential Electrical Mobility Analysis: A Theoretical Study', *Aerosol Sci. & Technol., 26*, 368-383.

Swietlicki, E., Hansson, H. C., Hameri, K., Svenningsson, B., Massling, A., McFiggans, G., McMurry, P. H., Petaja, T.,Tunved, P., Gysel, M., Topping, D., Weingartner, E., Baltensperger,U., Rissler, J., Wiedensohler, A., and Kulmala, M., 2008, Hygroscopic properties of submicrometer atmospheric aerosol particles measured with H-TDMA instruments in various environments – a review, *Tellus*, *60B*, 432–469.

Takahashi, K., 1971, Numerical veri_cation of Boltzman's distribution for electrical charge of aerosol particles. *J. Colloid & Interface Science*, *35*, 508-510.

Takeuchi, K., Yabumoto, J., Okada, Y., Kawai, T., Montajir, R. M., Goto, Y., 2005, A New Dual-Type DMA for Measuring Nanoparticles Emitted from Combustion Engines, *J. Nanoparticle Res.*, 7:287–293.

Tang, I. N. and Munkelwitz, H. R., 1993, Composition and temperature dependence of the deliquescence properties of hygroscopic aerosols, *Atmos. Environ., 27A*, 467–473.

Tammet, H., 1970, The aspiration method for the determination of atmospheric ion 645 spectra (Vol. II). Jerusalem: Israel program for scientific translations.

Tammet, H., Mirme, A., Tamm., E., 1998, Electrical Aerosol Spectrometer of Tartu University, *J. Aerosol Sci.,29:* S427-S428.

Tammet, H., Mirme, A., Tamm., E., 2002, Electrical aerosol Spectrometer of Tartu University, *Atmospheric Research, 62*:315-324.

Tarantola, A., 2005, *Inverse problem theory and methods for model parameter estimation*, SIAM, Philadelphia.

ten Brink, H.M., Plomp, A., Spoelstra, H., van de Vate, J.F., 1983, A High-Resolution Electrical Mobility Aerosol Spectrometer (MAS), *J. Aerosol Sci.14:*589-597.

Tikhonov, A.N., Arsenin, V.Y., 1977, *Solutions of Ill-posed Problems*, Winston & Sons, Washington, D.C.

Twomey, S. (1963) On the numerical solution of Fredholm integral equations of the Þrst kind by the inversion of the linear system produced by quadrature. *J. Ass. Comp. Mach*. 10, 97-101.

Twomey, S. (1975) Comparison of constrained linear inversion and an iterative non-linear algorithm applied to the indirect estimation of particle size distributions. *J. Comput. Phys*. 18, 188-200.

Twomey, S., 1977, *Introduction to the Mathematics of Inversion in Remote Sensing and Indirect Measurements*, Elsevier, New York.

Vogel, C. R. (1996) Non-convergence of the L-curve regularisation parameter selection method. *Inverse Problems* 12, 535-547.

Voutilainen, A., Kolehmainen, V., Kaipio, J.P., 2000, Statistical inversion of aerosol size measurement data, University of Kuopio.

Wahba, G. (1977) Practical approximate solutions to linear operator equations when the data are noisy. *SIAM J. Numer. Anal*. 14, 651-667

Walter, J., 2001, "Size Distribution Characteristics of Aerosols", in *Aerosol Measurements: Principles, Techniques, and Applications*, Second Edition, Baron, A. and Willeke, K. (Eds.), Wiley-InterScience, New York.

Wang, S.C., Flagan, R.C., 1990, Scanning Electrical Mobility Spectrometer, *Aerosol 647 Sci. & Technol.*,13:230-240.

Weingartner, E., Gysel, M., Baltensperger, U., 2002, Hygroscopicity of aerosol particles at low temperatures. 1. New low-temperature H-TDMA instrument: Setup and first applications. *Environmental Science and Technology*, *36*: 55–62.

Whitby, K.T., Clark, W.E., 1966, Electric aerosol particle counting and size distribution measuring system for the 0.015 to 1 μ size range, *Tellus, 2*: 573-586.

White, H. J. 1951. *AIEE Trans*. 70:1186-1191.

Winklmayr, W., Wang, H. C. and John, W. (1990) Adaptation of the Twomey algorithm to the inversion of cascade impactor data. *Aerosol Sci*. T*echnol*. 13, 322-331.

Winklmayr, W., Reischl, G.P., Lindner, A.O., Berner, A., 1991, A New Electromobility Spectrometer for the Measurement of Aerosol Size Distributions in the Size Range from 1 to 1000 nm, *J. Aerosol Sci. 22:* 289-296.

Yee, E. (1989) On the interpretation of diffusion battery data. *J. Aerosol Sci*. 20, 797-811.

Zhang, S.H., Akutsu, Y., Russell, L.M. , Flagan, R. C., Seinfeld, J. H.,1995, Radial 649 Differential Mobility Analyzer, *Aerosol Sci. & Technol.*, 23: 357- 372.

Zhang, S.H., Flagan, R.C., 1996, Resolution of the Radial Differential Mobility 651 Analyzer for Ultrafine Particles, *J. Aerosol Sci*., 27:1179-1200

Zhang, K.M, Wexler, A.S., 2006, An asynchronous time-stepping (ATS) integrator for atmospheric applications: Aerosol dynamics, *Atmospheric Env. 40*: 4574-4588.

Zeleny, J. (1929). The distribution of mobilities of ions in moist air. *Physical Review*, *34*, 310-334.